



TAUP 2023

Vienna, 28 August-1 September 2023



Probing the Blue Axion with Cosmic Optical Background Anisotropies

Giuseppe LUCENTE

(University of Heidelberg, Bari University & INFN)

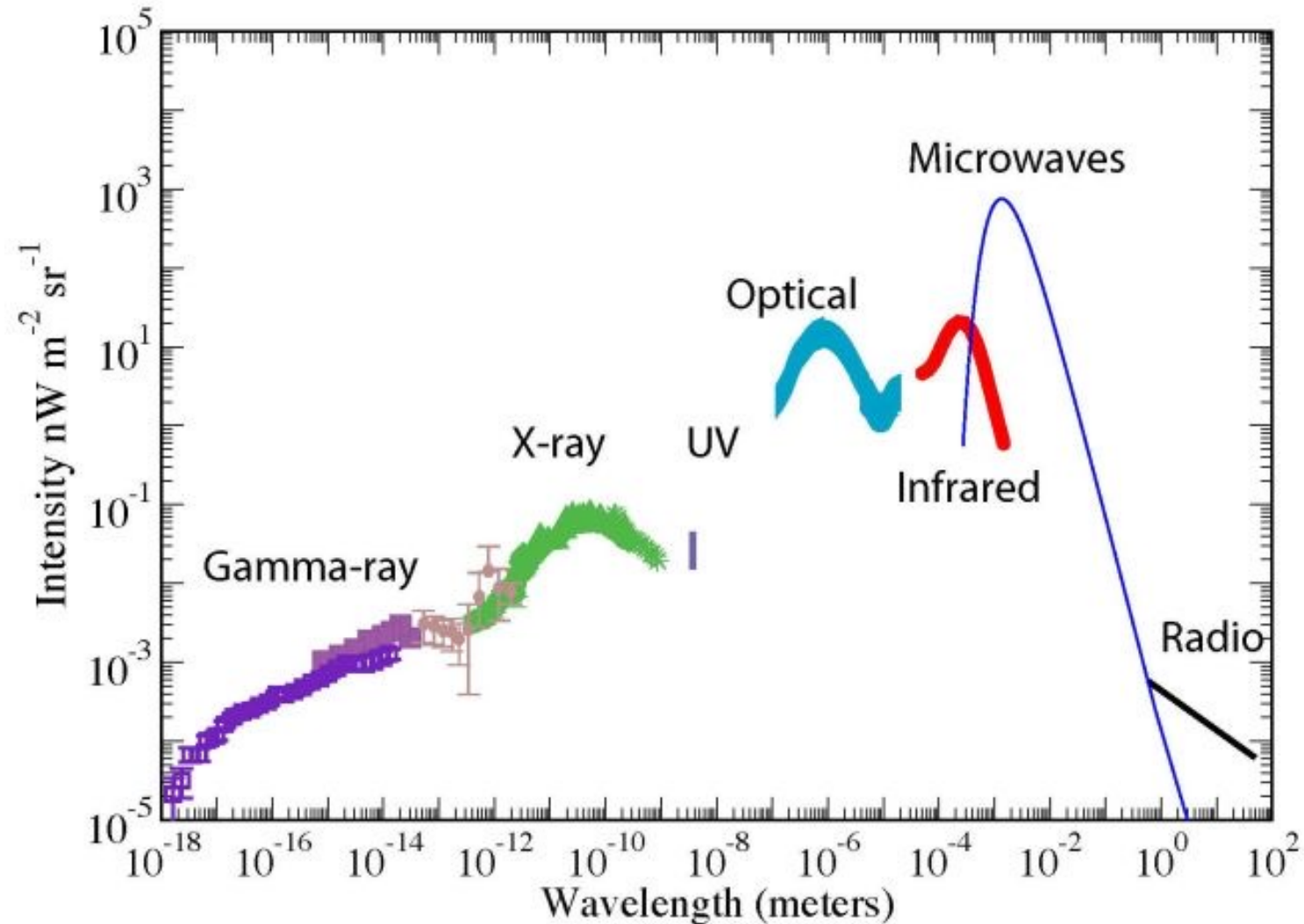
Based on

P. Carena, GL, E. Vitagliano, PRD 107 (2023) 8, 083032, arXiv: 2301.06560

This project has received funding /support from the European Union's Horizon 2020 research and innovation programme under the Marie Skłodowska-Curie grant agreement No 860881-HIDDeN

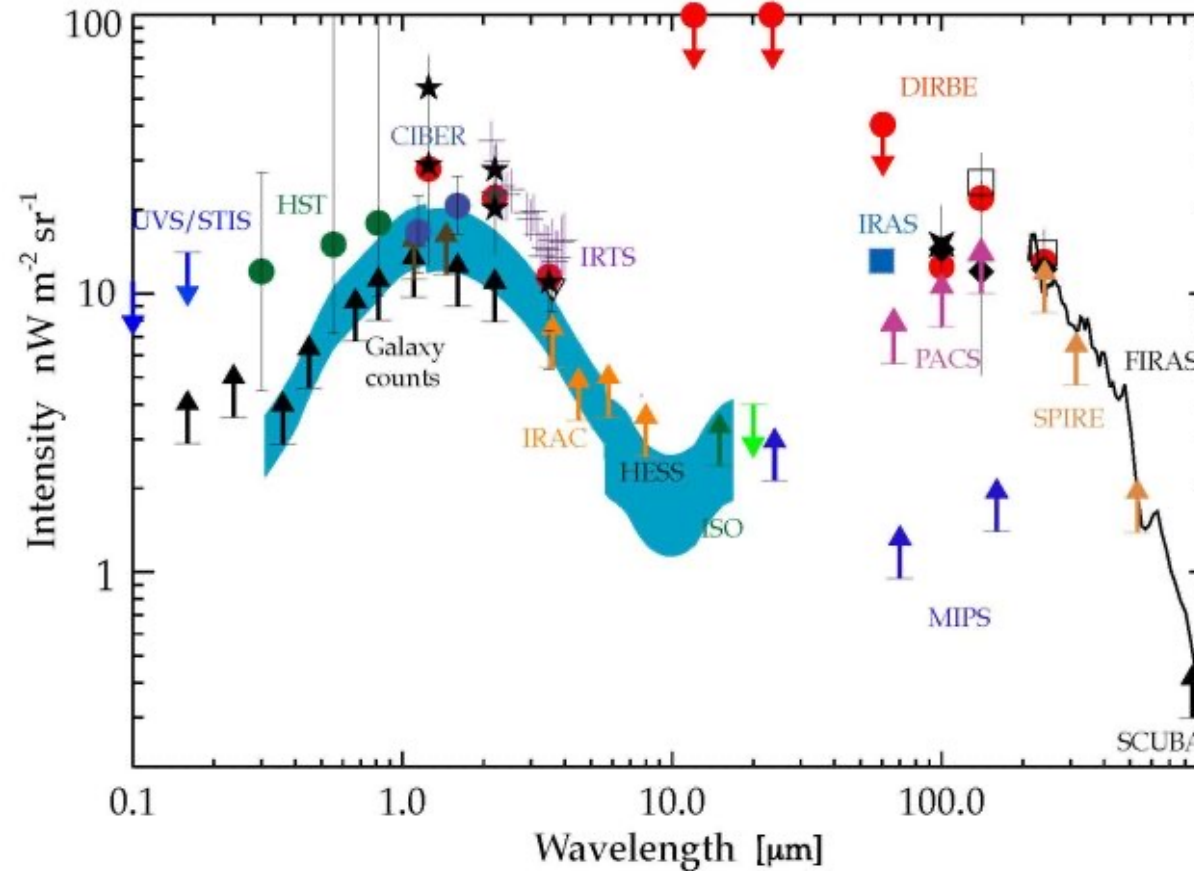
THE EXTRAGALACTIC BACKGROUND LIGHT

[A. Cooray, ArXiv:1602.03512]



THE COSMIC OPTICAL BACKGROUND

[A. Cooray, ArXiv:1602.03512]



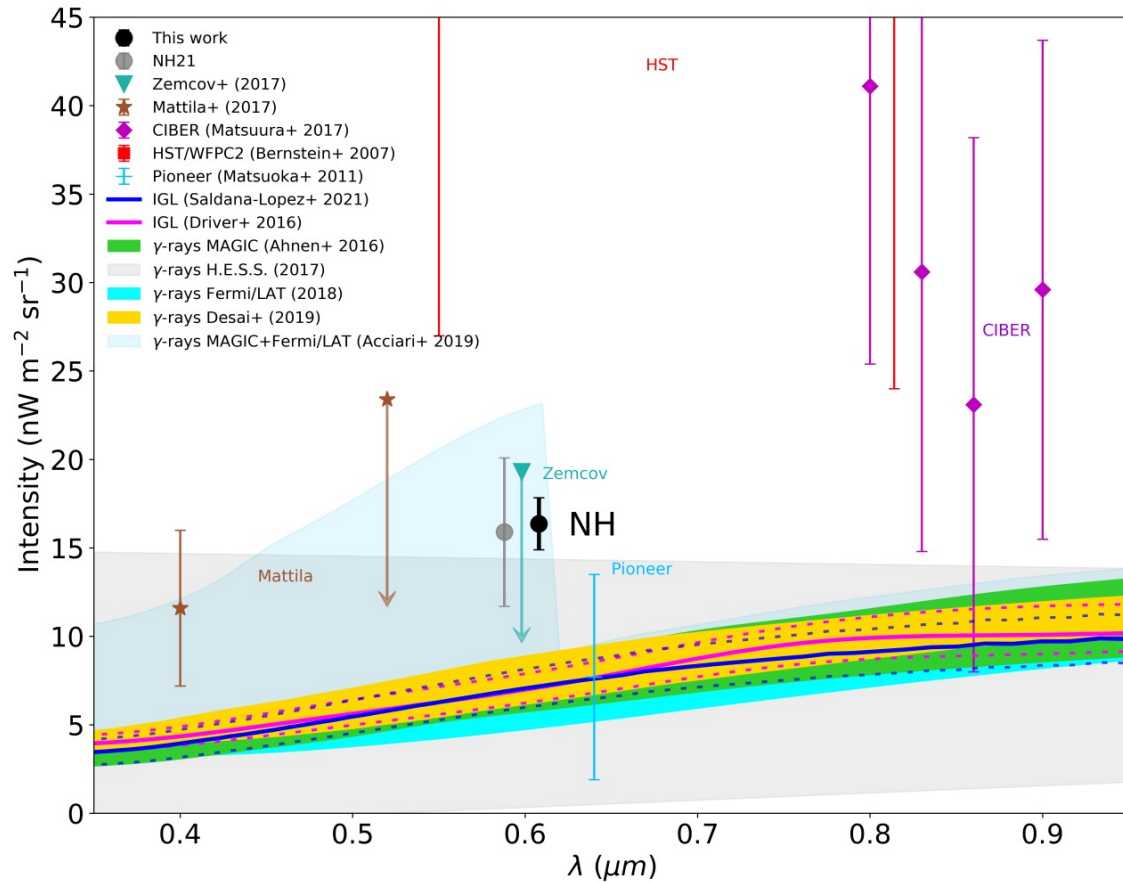
The COB can be estimated via

- Direct detection [Pioneer, New Horizon]
- Galaxy counts [Hubble Space Telescope (HST)]
- Analysis of observed blazar spectra [HESS, MAGIC]

COB EXCESS MEASURED BY LORRI

[T. Lauer et al., *Astrophys. J. Lett* 927 (2022) 1, L8]

The COB measured by New Horizons LORRI is 4σ larger than expected.



$$I = 16.37 \pm 1.47 \text{ nW m}^{-2} \text{sr}^{-1}$$

$$\lambda = 0.608 \mu\text{m}$$

51.3 A.U. from the Sun

Possible explanations: high redshift galaxies, direct-collapse black holes, zodiacal light (not convincing...)

AXION EXPLANATION OF THE COB EXCESS

[J.L. Bernal et al., PRL 129 (2022) 23, 231301]

LORRI excess can be explained via dark matter axions decaying to monoenergetic photons.

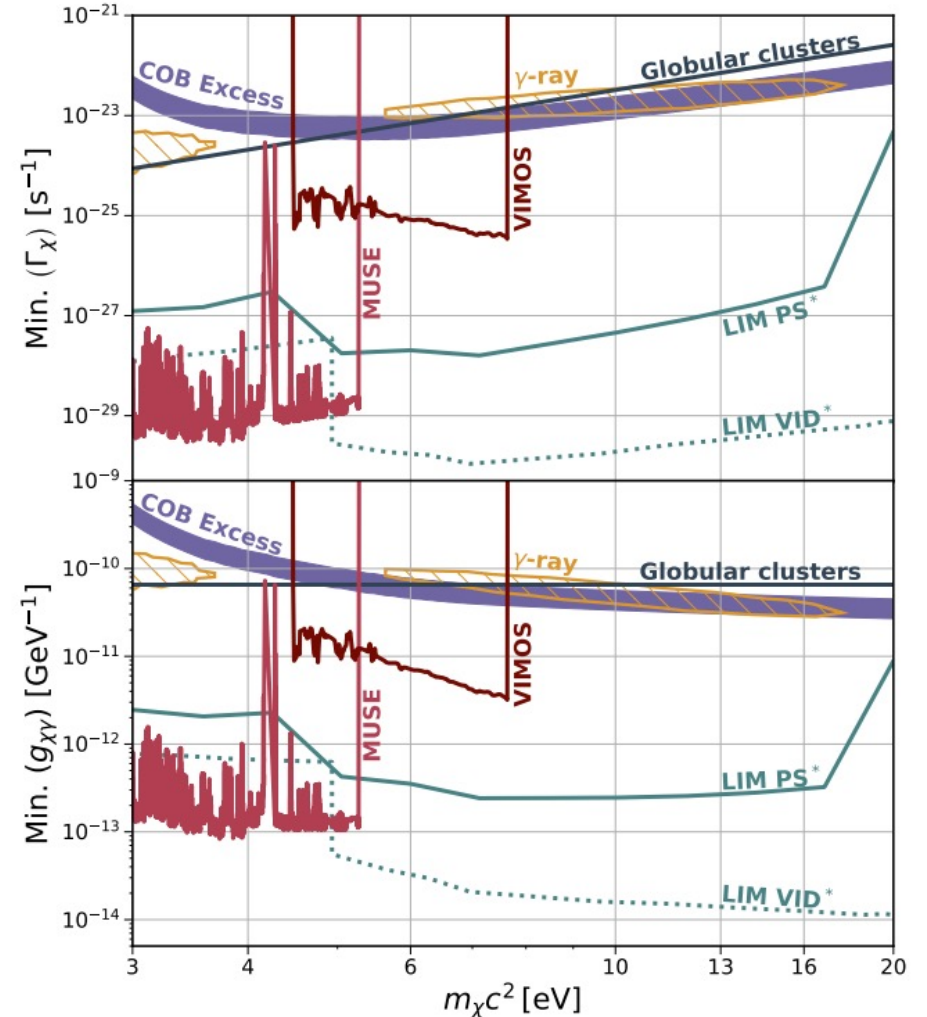
$$\mathcal{L}_{a\gamma} = \frac{1}{4} g_{a\gamma} a F_{\mu\nu} \tilde{F}^{\mu\nu}$$

Decay rate $\Gamma_{a\gamma} = \frac{g_{a\gamma}^2}{64\pi} m_a^3$

Contribution to COB from decaying DM axions with

$$m_a \sim 10 \text{ eV} \left(\nu = \frac{m_a}{2} \right):$$

- QCD axion ruled out by observations.
- Excess due to axion-like particles decaying to blue and UV light (blue axions).



AXION CONTRIBUTION TO COB

[O.E. Kalashev et al., PRD 99 (2019) 2, 023002]

- Average intensity from decaying DM particles

$$\langle I(\omega) \rangle = \frac{\omega^2}{4\pi} \frac{dN_\gamma}{dS d\omega dt} = \frac{\omega}{4\pi} \frac{\rho_a}{m_a} \frac{2 \Gamma_{a \rightarrow \gamma\gamma}}{H \left(\frac{m_a}{2\omega} - 1 \right)}$$

- DM density fluctuations: anisotropies in the decay-product photon flux.

$$\delta I(\omega_{\text{piv}}, \hat{\mathbf{n}}) = I(\omega_{\text{piv}}, \hat{\mathbf{n}}) - \langle I(\omega_{\text{piv}}) \rangle = \sum_{l,m} a_{lm}(\omega_{\text{piv}}) Y_{lm}(\hat{\mathbf{n}})$$

$I(\omega_{\text{piv}}, \hat{\mathbf{n}})$ intensity seen by the detector pointing at the direction $\hat{\mathbf{n}}$ in the sky.

ANGULAR POWER SPECTRUM

Correlations over each multipole moment l given by

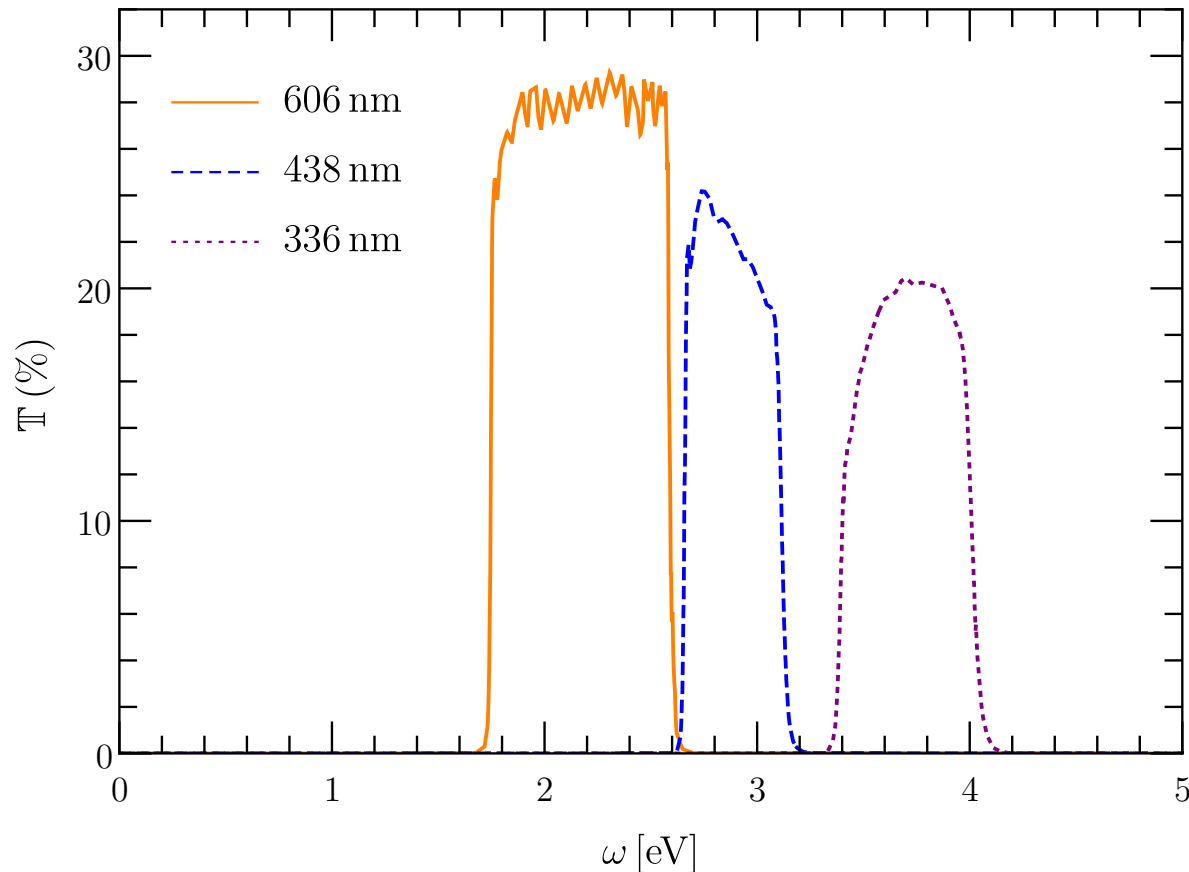
$$C_l(\omega_{\text{piv}}) = \left\langle |a_{lm}(\omega_{\text{piv}})|^2 \right\rangle = \frac{1}{2l+1} \sum_{m=-l}^{+l} |a_{lm}(\omega_{\text{piv}})|^2 =$$

$$\int_0^\infty dz \left[\frac{1}{4\pi} \frac{2 \omega_{\text{piv}}^2}{m_a H(z)} \frac{\rho_a}{m_a} 2 \Gamma_{a \rightarrow \gamma\gamma} \right]^2 \left[\epsilon \left(\frac{m_a}{2(1+z)} \right) \right]^2 \frac{H(z)}{r(z)^2} P_\delta \left[k = \frac{l}{r(z)}, r(z), r(z) \right]$$

- ϵ detector normalized throughput
- ω_{piv} detector pivot wavelength
- P_δ DM power spectrum
- ρ_a DM abundance

ANISOTROPY MEASUREMENTS

The available shortest wavelength HST measurements are at 606 nm.



$$\epsilon(\omega) = \frac{T(\omega)}{\int_0^{\infty} \frac{d\omega}{\omega} T(\omega)}$$

Filter	ω_{pivot} (eV)	Efficiency
F336W	3.70	0.0313
F438W	2.87	0.0347
F606W	2.11	0.1093

[<https://www.stsci.edu/hst/instrumentation/wfc3>]

Stronger constraints can be obtained with future observations at shorter wavelengths.

POSSIBLE PRODUCTION MECHANISMS

COLD DARK MATTER

- Misalignment: eV-ish QCD axion excluded by astrophysical arguments. [J. Preskill et al., PLB 120 (1983)]
- Topological defect decay: reasonable for axion-like particles. [C.A.J. O'Hare et al., PRD 105 (2022) 055025]

POSSIBLE PRODUCTION MECHANISMS

COLD DARK MATTER

- Misalignment: eV-ish QCD axion excluded by astrophysical arguments. [J. Preskill et al., PLB 120 (1983)]
- Topological defect decay: reasonable for axion-like particles. [C.A.J. O'Hare et al., PRD 105 (2022) 055025]

NON-COLD DARK MATTER

Thermalization process: Primakoff effect $\gamma Q \rightarrow Qa$. [D. Cadamuro, ArXiv: 1210.3196]

- Freeze-out $T_F \approx 4 \times 10^4 \text{ GeV} \left(\frac{g_{a\gamma}}{10^{-11} \text{ GeV}^{-1}} \right)^{-2} \rightarrow T_F > \Lambda_{\text{EW}}$ for $g_{a\gamma} \lesssim 10^{-9} \text{ GeV}^{-1}$
[E.W. Kolb & M.S. Turner, Nature 294 (1981) 521]

$$\Omega_a h^2 = \frac{m_a}{13 \text{ eV}} \frac{1}{g_{*,s}(T_F)} \quad \frac{T_a}{T_0} = \left(\frac{g_*(T_0)}{g_{*,s}(T_F)} \right)^{1/3} \quad T_0 \text{ CMB temperature}$$

- Freeze-in: Negligible contribution [K. Langhoff, PRL 129 (2022) 241101]

$$\Omega_a h^2 = 10^{-5} \left(\frac{m_a}{\text{eV}} \right) \left(\frac{g_{a\gamma}}{10^{-8} \text{ GeV}^{-1}} \right)^2 \left(\frac{T_{\text{RH}}}{5 \text{ MeV}} \right)$$

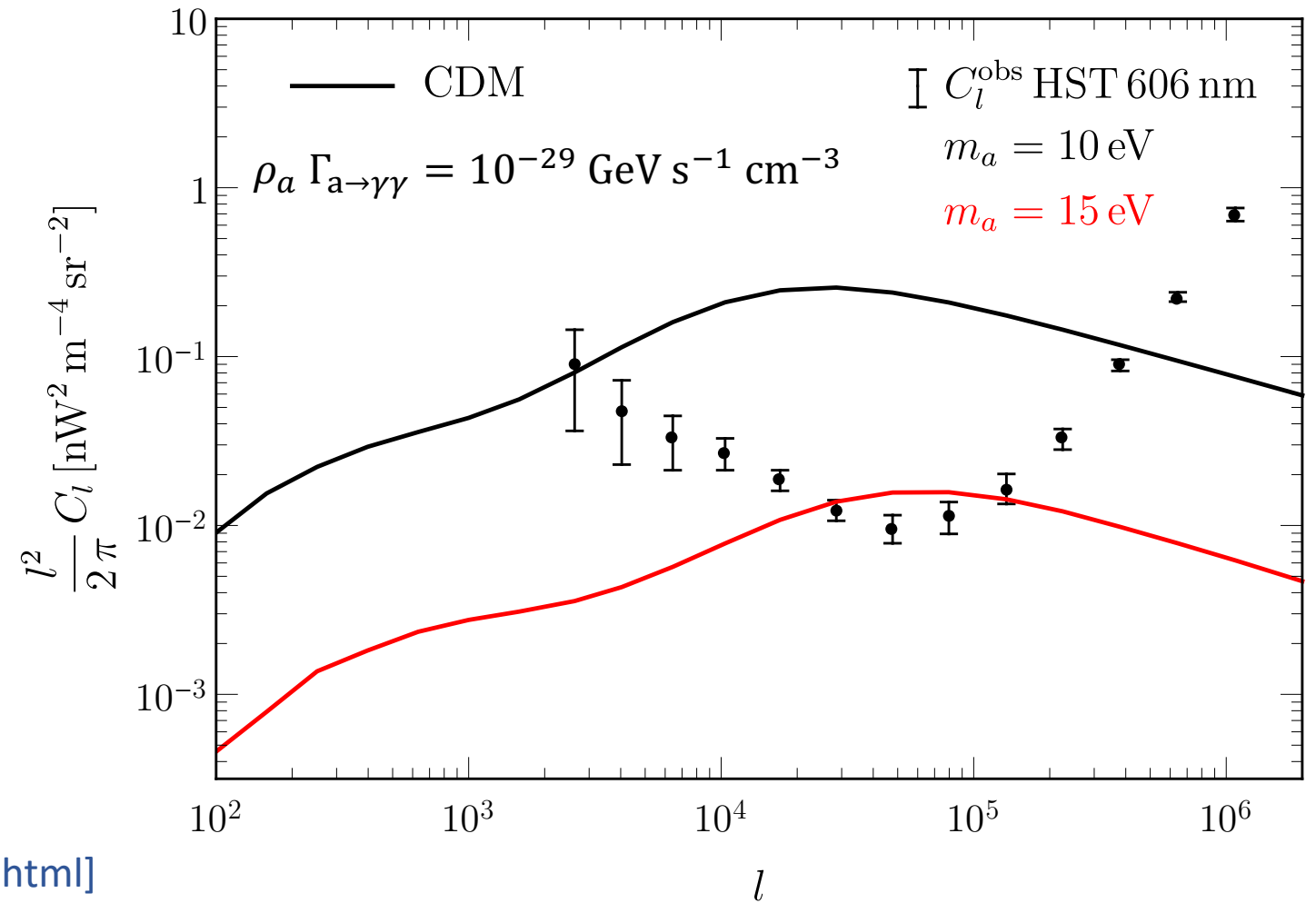
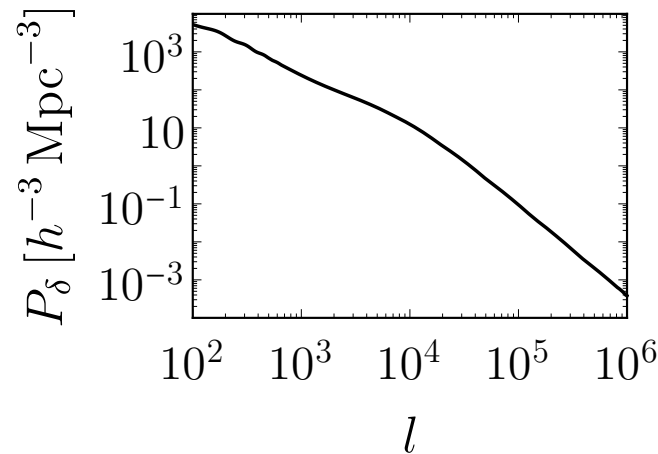
ANGULAR POWER SPECTRUM FOR CDM

The angular power spectrum can be computed fixing the value of

- CDM abundance

$$\rho_a = \Omega_{\text{CDM}} \rho_c, \quad \Omega_{\text{CDM}} h^2 = 0.12$$

- CDM non-linear power spectrum



[https://lesgourg.github.io/class_public/class.html]

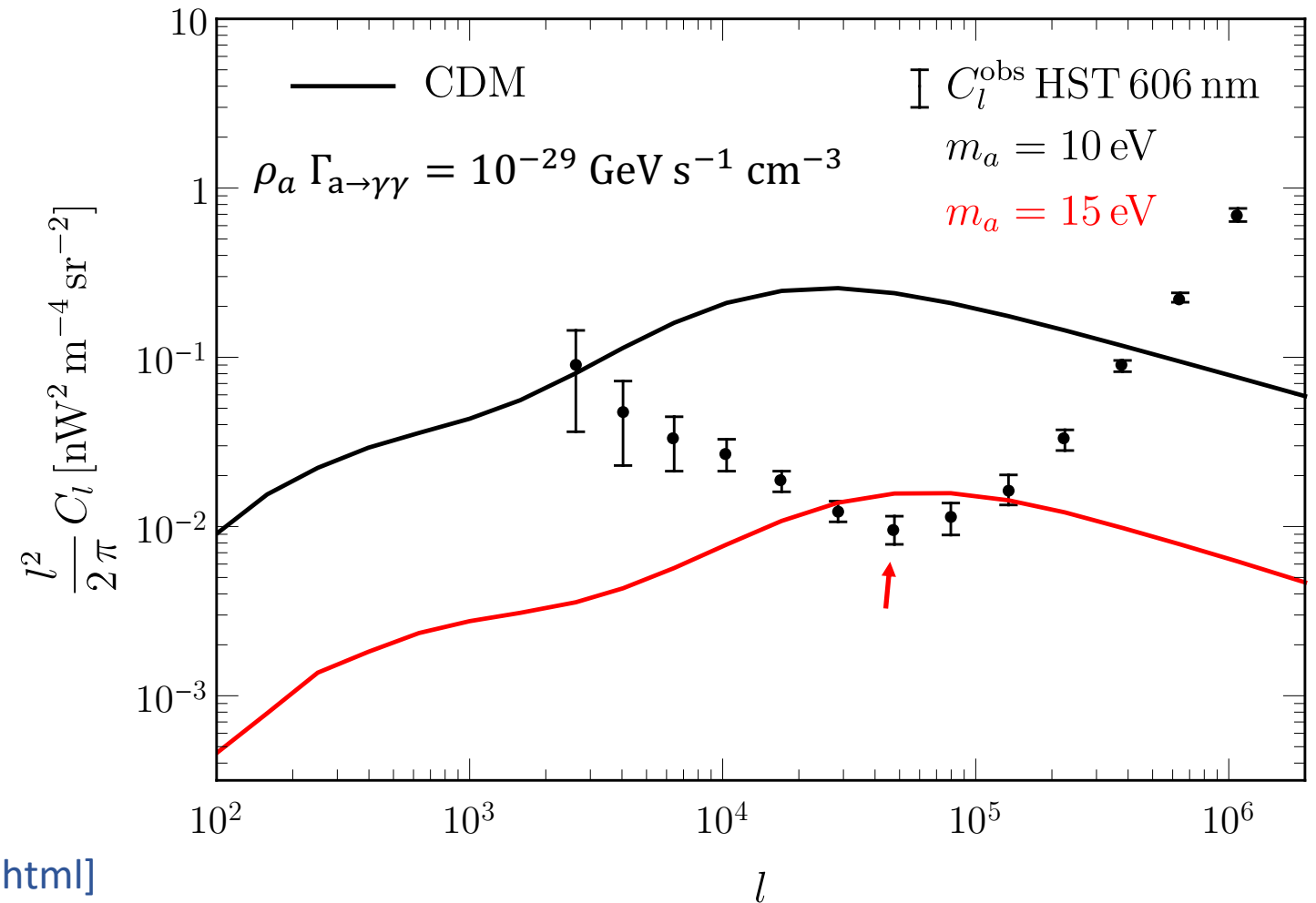
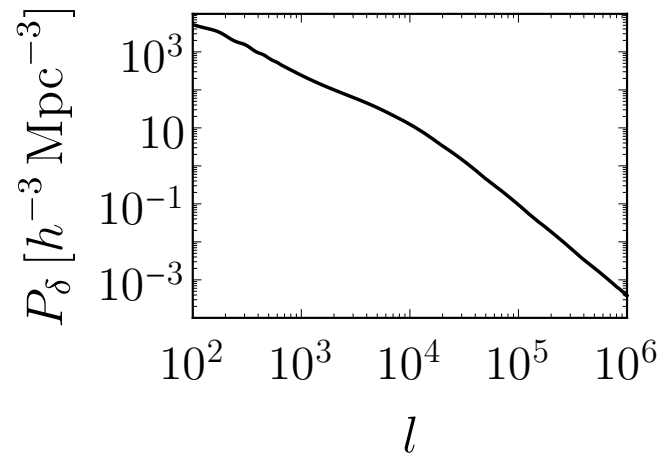
ANGULAR POWER SPECTRUM FOR CDM

The angular power spectrum can be computed fixing the value of

- CDM abundance

$$\rho_a = \Omega_{\text{CDM}} \rho_c, \quad \Omega_{\text{CDM}} h^2 = 0.12$$

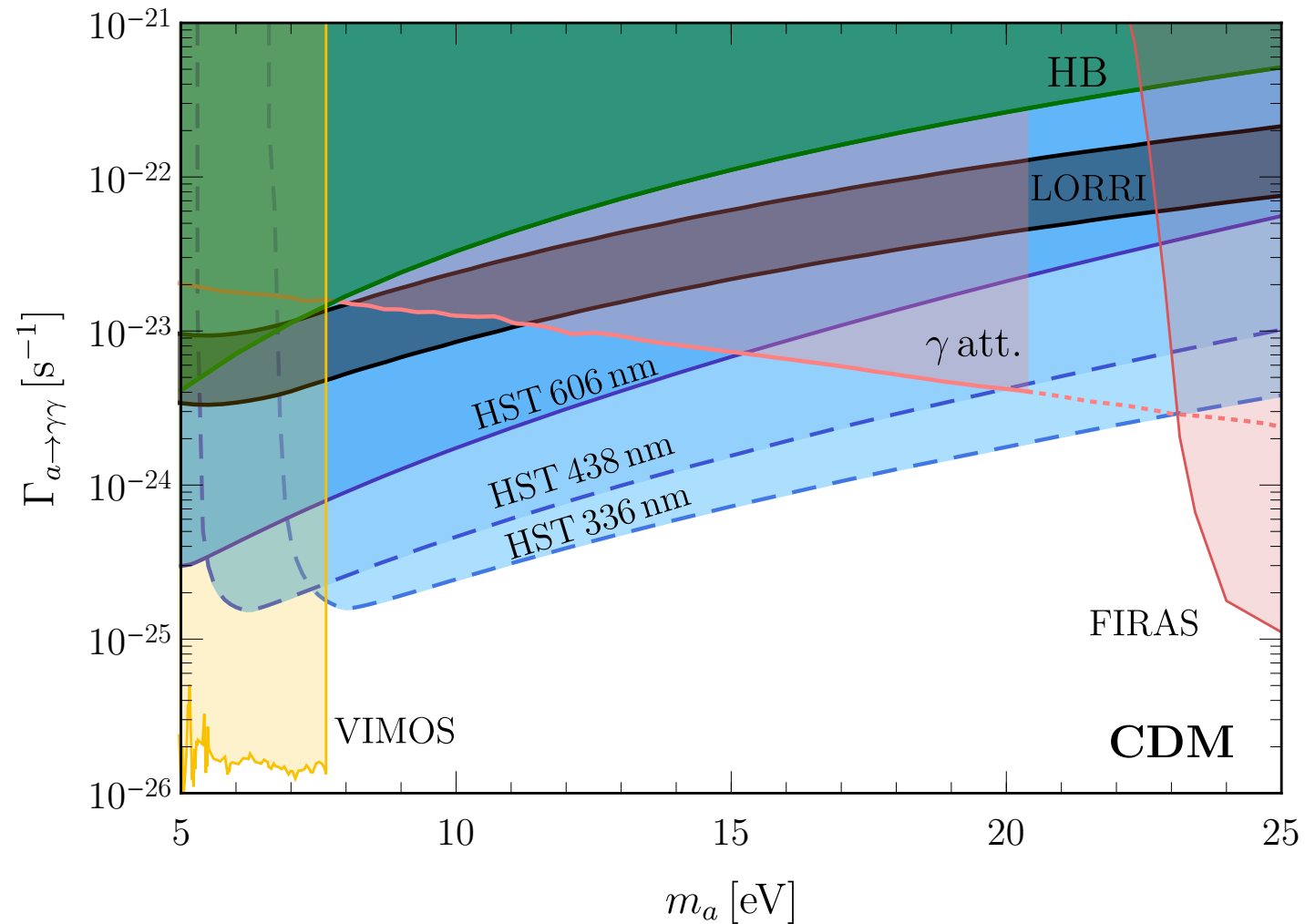
- CDM non-linear power spectrum



[https://lesgourg.github.io/class_public/class.html]

The angular power spectrum must not exceed the upper bar of any data points.

BOUNDS AND REACHES ON CDM AXION



HST measurements at 606 nm exclude LORRI hint, in agreement with [K. Nakayama & W. Yin, PRD 106 (2022)]

Future measurements would improve the bound by one order of magnitude.

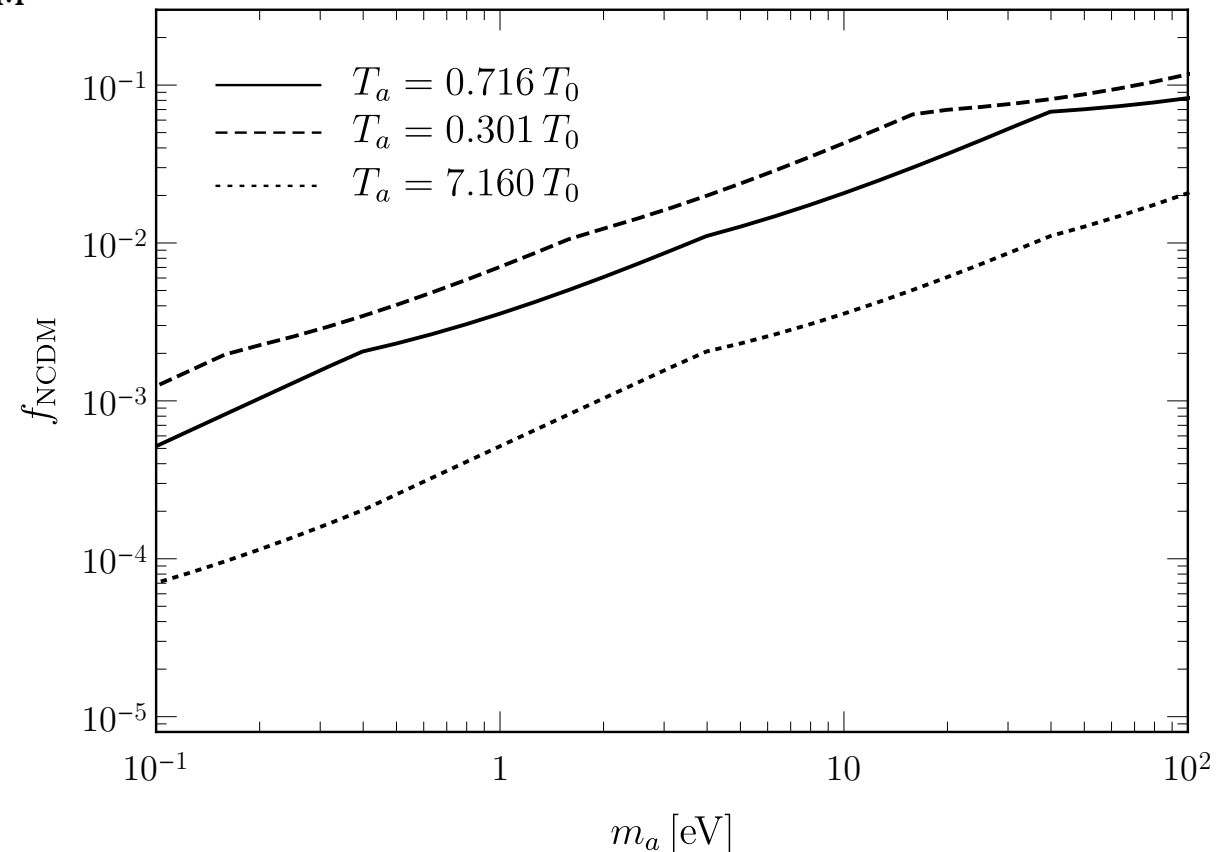
NON-COLD DARK MATTER

[E.W. Kolb & M.S. Turner, Nature 294 (1981) 521]

$$\Omega_a h^2 = \frac{m_a}{13 \text{ eV}} \frac{1}{g_{*,s}(T_F)} \quad \frac{T_a}{T_0} = \left(\frac{g_*(T_0)}{g_{*,s}(T_F)} \right)^{1/3}$$

Structure formation constraints imply $f_{\text{NCDM}} = \frac{\Omega_{\text{NCDM}}}{\Omega_{\text{CDM}}} \ll 1$. [R. Diamanti et al., JCAP 06 (2017) 008]

For $m_a \sim 10 \text{ eV}$, $g_{*,s}(T_F > \Lambda_{\text{EW}}) = 106.75$:
 $\Omega_a \gg f_{\text{NCDM}} \Omega_{\text{CDM}}$



NON-COLD DARK MATTER

[E.W. Kolb & M.S. Turner, Nature 294 (1981) 521]

$$\Omega_a h^2 = \frac{m_a}{13 \text{ eV}} \frac{1}{g_{*,s}(T_F)} \quad \frac{T_a}{T_0} = \left(\frac{g_*(T_0)}{g_{*,s}(T_F)} \right)^{1/3}$$

Structure formation constraints imply $f_{\text{NCDM}} = \frac{\Omega_{\text{NCDM}}}{\Omega_{\text{CDM}}} \ll 1$. [R. Diamanti et al., JCAP 06 (2017) 008]

For $m_a \sim 10 \text{ eV}$, $g_{*,s}(T_F > \Lambda_{\text{EW}}) = 106.75$:
 $\Omega_a \gg f_{\text{NCDM}} \Omega_{\text{CDM}}$

1. Modified freeze-out

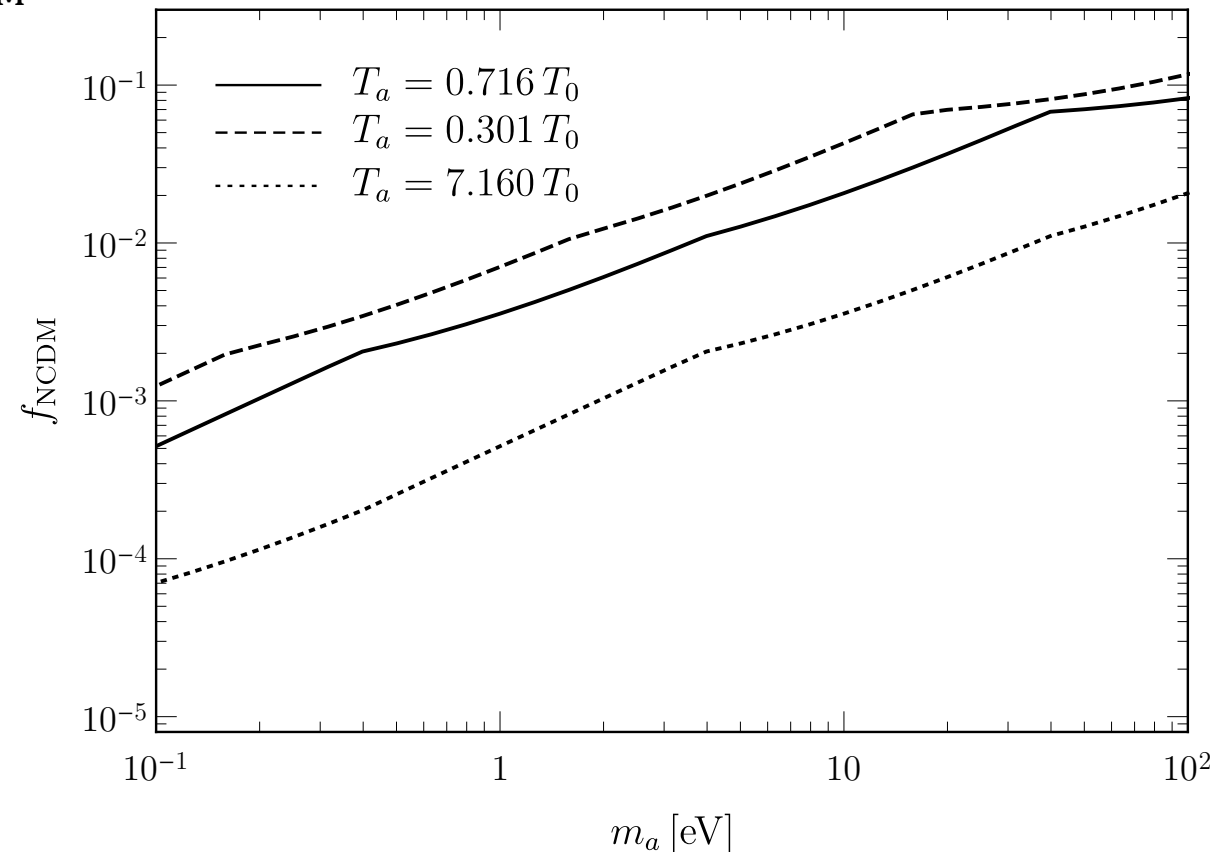
Additional degrees of freedom to increase $g_{*,s}$:
 $\Omega_a h^2 = f_{\text{NCDM}} \Omega_{\text{CDM}} h^2$.

2. Hot relic

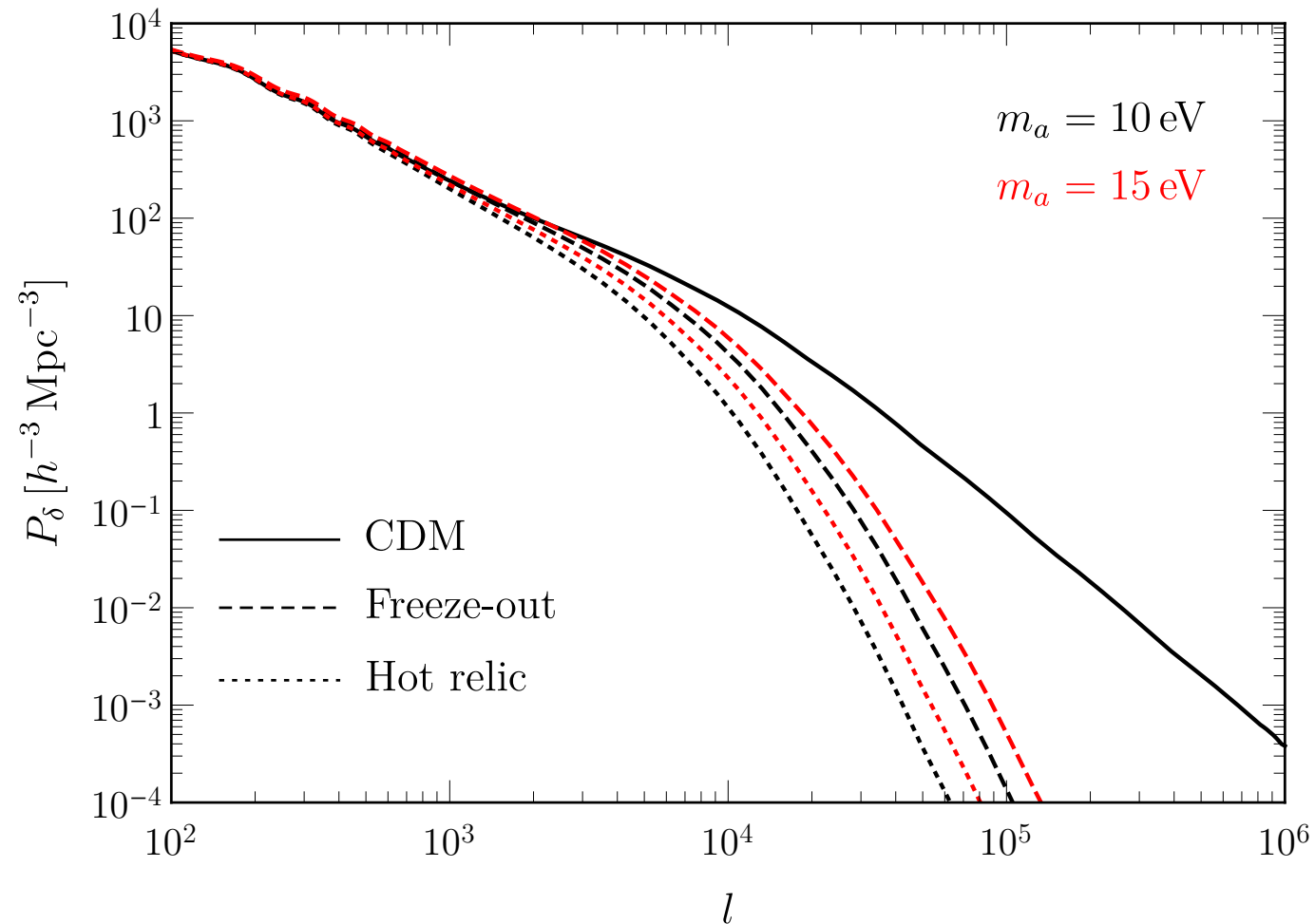
Axions with:

$$T_a = T_\nu = 0.716 T_0,$$

Ω_a saturating structure formation bounds.

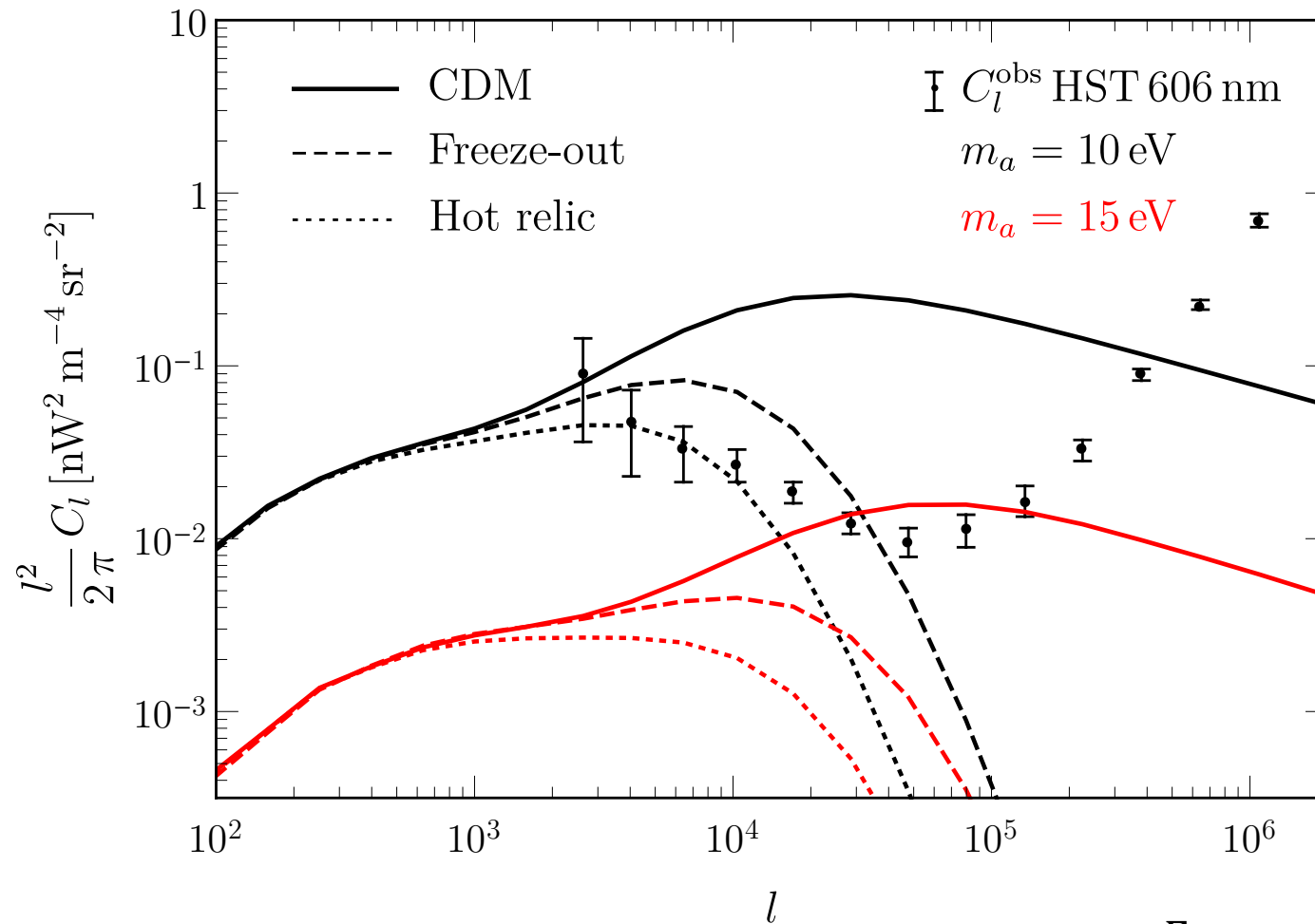


THE ROLE OF THE POWER SPECTRUM



The power spectrum is suppressed at larger scales for hotter DM.

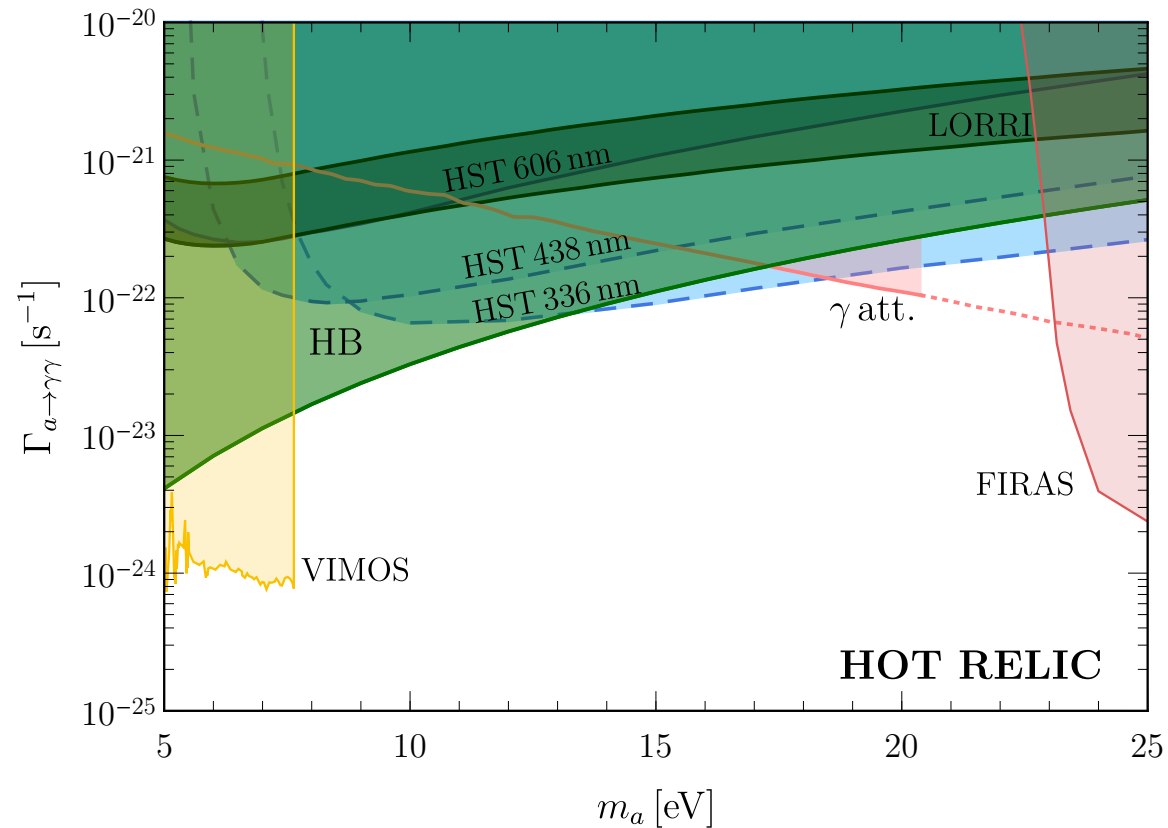
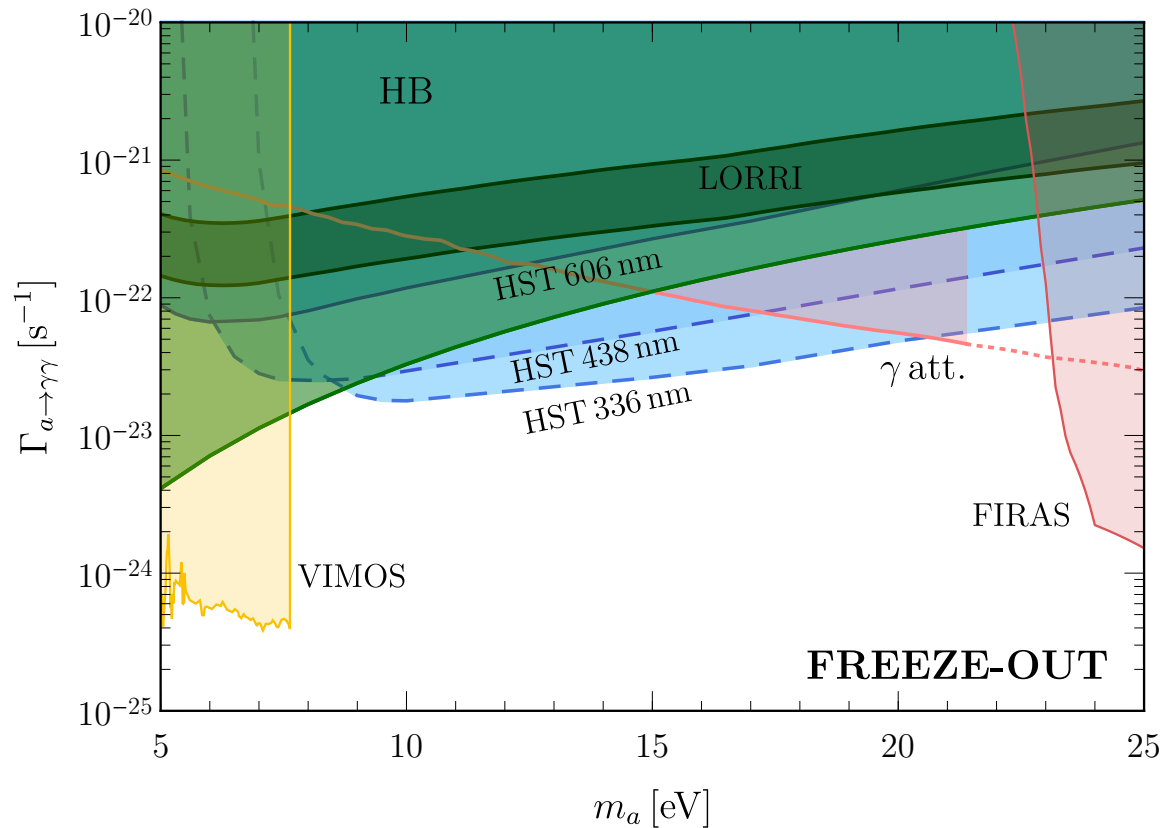
OBSERVED ANGULAR POWER SPECTRUM



$$\rho_a \Gamma_{a \rightarrow \gamma\gamma} = 10^{-29} \text{ GeV s}^{-1} \text{ cm}^{-3}$$

The hot relic case is the most conservative scenario.

BOUNDS ON NCDM

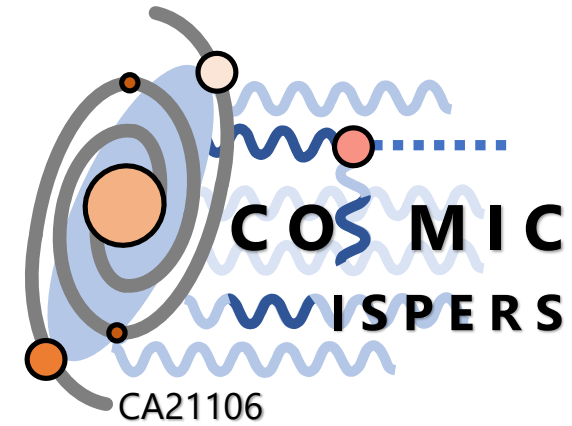


LORRI hint excluded also for NCDM.

Strongest probe for $m_a \sim 15$ eV from future measurements.

CONCLUSIONS

- COB measurements are efficient tools to probe eV-ish axions.
- Anisotropy measurements from HST exclude the interpretation of the LORRI excess as decaying DM axion.
- Bounds are robust ($C_l \sim \Gamma_{a\gamma}^2 \sim g_{a\gamma}^4$) and can be slightly strengthened by fitting HST data with additional contributions.
- Future measurements will explore a current unconstrained region: possibility to detect signals from blue axions.



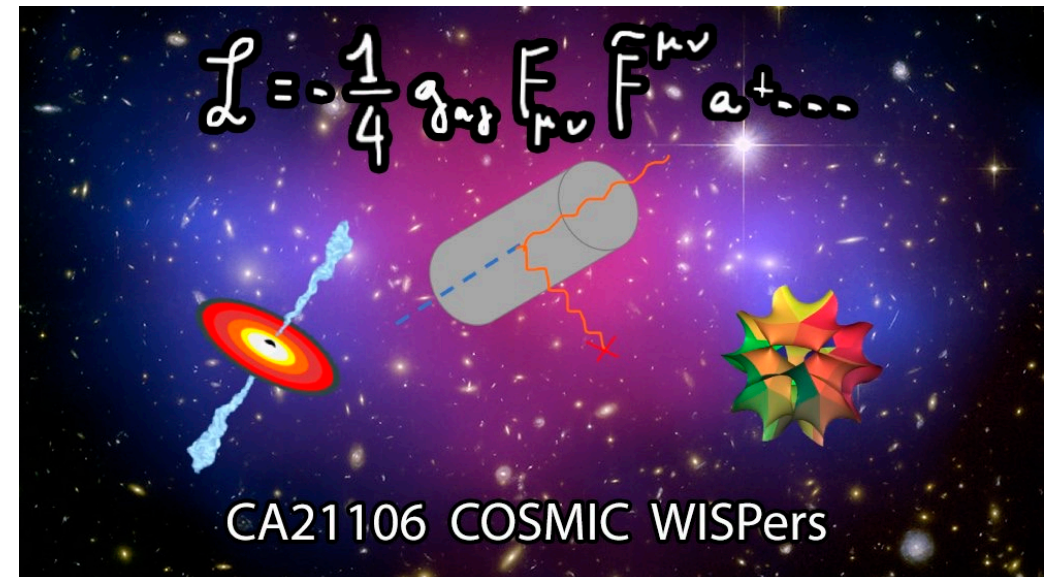
COST ACTION CA21106

COSMIC WISPERS in the Dark Universe: Theory, Astrophysics and Experiments

More info at <https://www.cost.eu/actions/CA21106/>

General Meeting 05-08 September 2023
<https://agenda.infn.it/event/34125/>

Training School 11-14 September 2023
<https://agenda.infn.it/event/34190/>



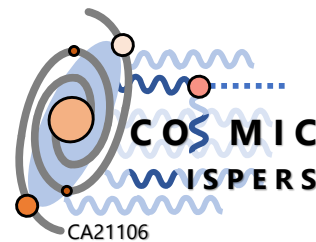


UNIVERSITÄT
HEIDELBERG
ZUKUNFT
SEIT 1386



Thank you for your attention

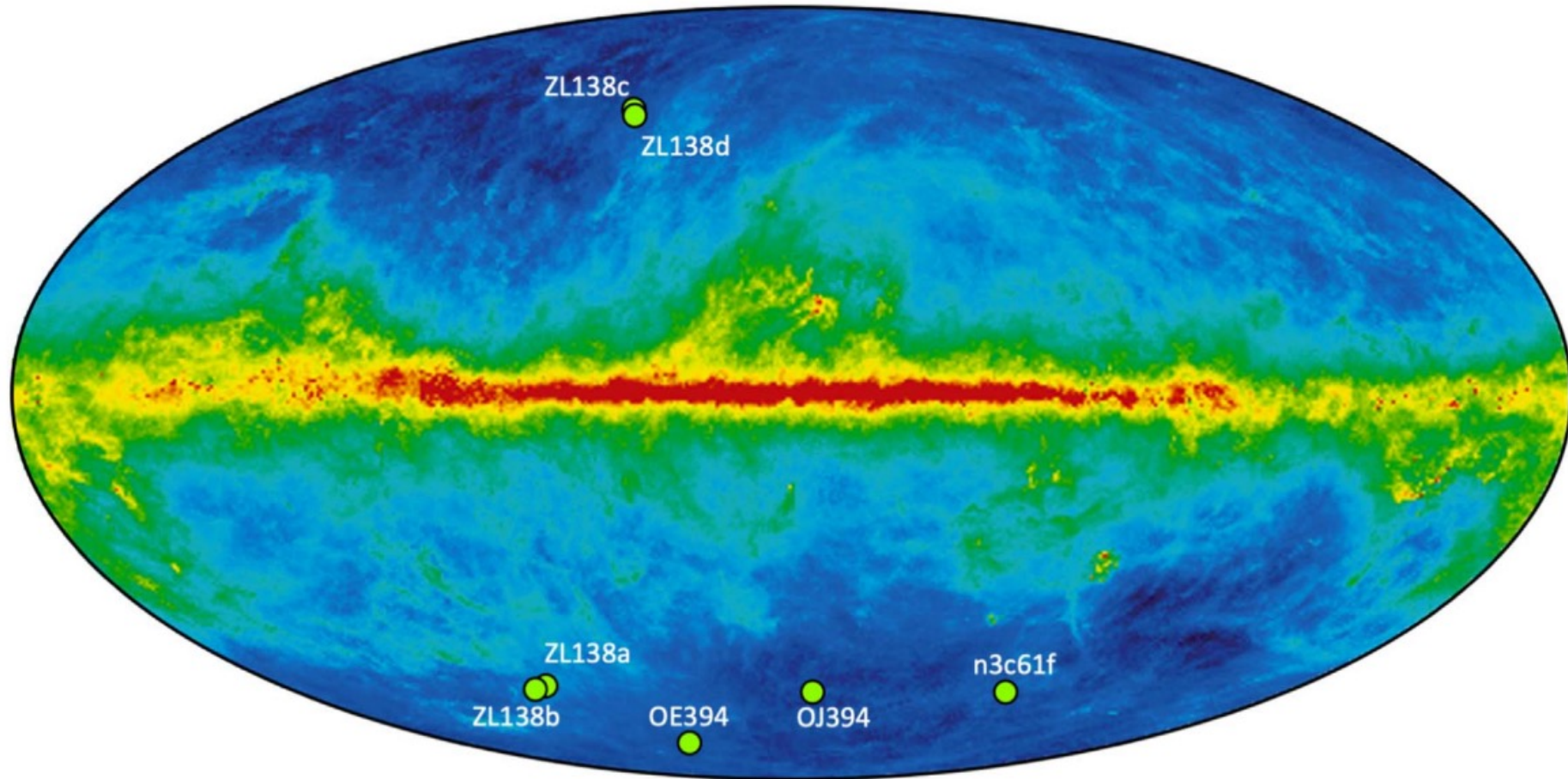
Email address: giuseppe.lucente@ba.infn.it



UNIVERSITÀ
DEGLI STUDI DI BARI
ALDO MORO

THE COSMIC OPTICAL BACKGROUND

[T. Lauer et al., *Astrophys. J. Lett* 906 (2021) 77]



THE COB FOREGROUNDS

[T. Lauer et al., *Astrophys. J. Lett* 906 (2021) 77]

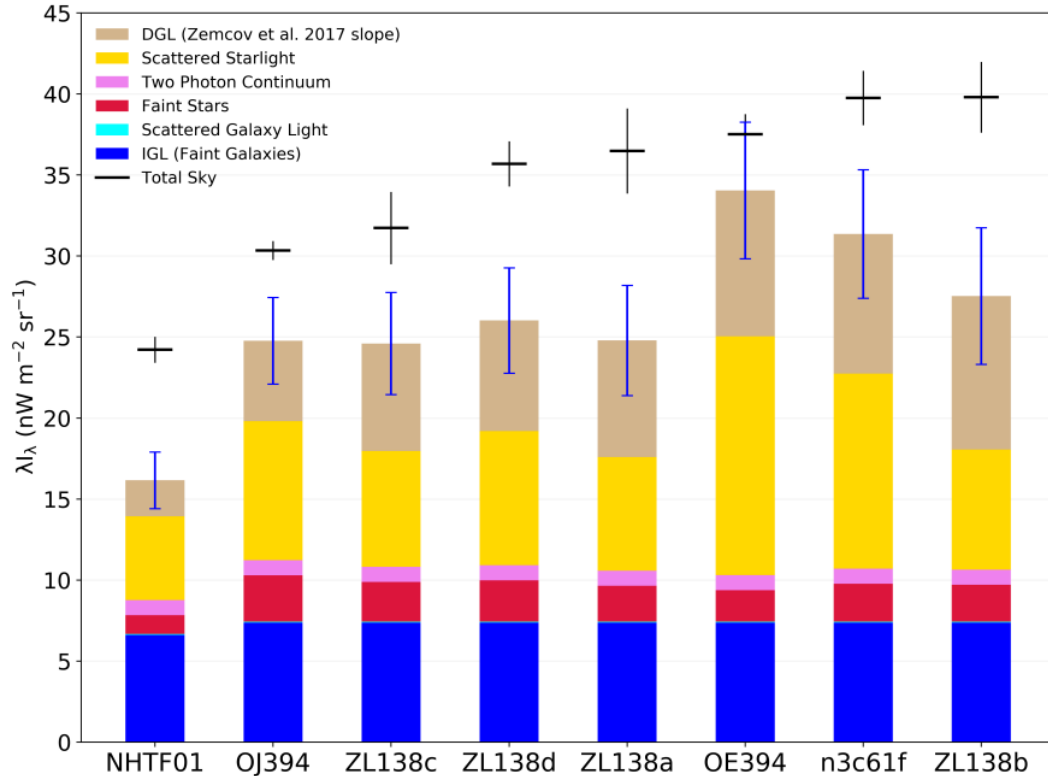


Table 1. Sky Flux Decomposition

Component	$\text{nW m}^{-2} \text{sr}^{-1}$	Stat.	Sys.
Total Sky	24.22 ± 0.80	0.80	0.00
– Scattered Starlight (SSL)	5.17 ± 0.52	0.00	0.52
– Scattered Milky Way Light (DGL)	2.22 ± 1.00	0.32	0.95
– Faint Stars (FSL)	1.16 ± 0.18	0.06	0.17
– Two-photon continuum (2PC)	0.93 ± 0.47	0.00	0.47
– Scattered Galaxy Light (SGL)	0.07 ± 0.01	0.00	0.01
+ Bright Field Galaxies	1.70 ± 0.07	0.04	0.06
= Cosmic Optical Background	16.37 ± 1.47	0.86	1.19
– Integrated Galaxy Light (IGL)	8.31 ± 1.24	0.78	0.97
= Anomalous Flux	8.06 ± 1.92	1.16	1.53

COMPUTATION OF THE ANGULAR POWER SPECTRUM

$$\langle I(\omega) \rangle = \omega^2 \int dz W[\omega(1+z), z] = \frac{\omega \rho_a}{4\pi m_a} \frac{2 \Gamma_{a \rightarrow \gamma\gamma}}{H\left(\frac{m_a}{2\omega} - 1\right)}$$

$$I(\omega_{\text{piv}}^2, \mathbf{n}) = \omega_{\text{piv}}^2 \int \frac{d\omega}{\omega} \int dz W[\omega(1+z), z, \mathbf{n}] \epsilon(\omega)$$

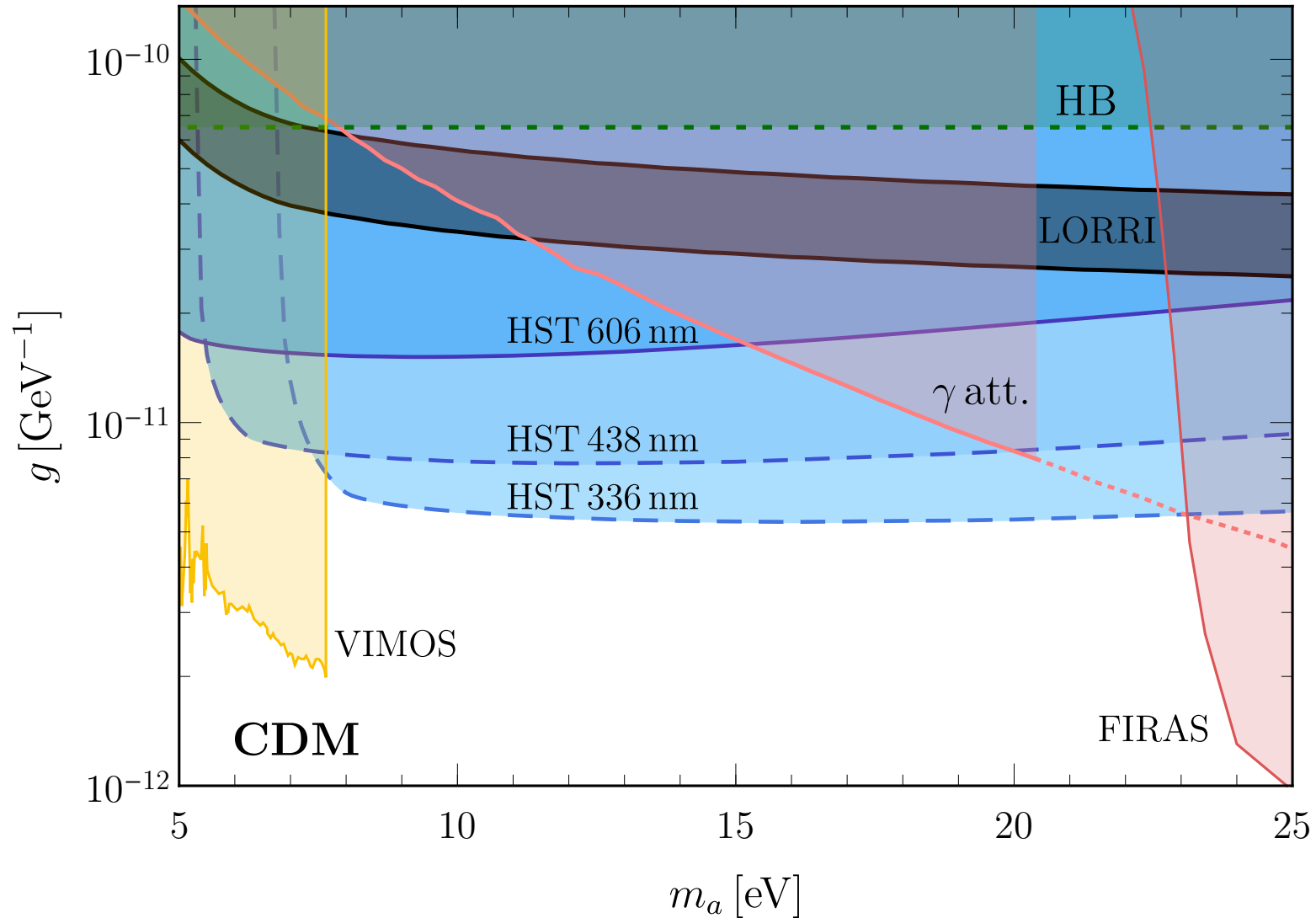
$$\begin{aligned} C_l(\omega_{\text{piv}}) &= \omega_{\text{piv}}^2 \int \frac{d\omega_1}{\omega_1} \epsilon(\omega_1) \int dz_1 W[\omega_1(1+z_1), z_1] \\ &\quad \times \omega_{\text{piv}}^2 \int \frac{d\omega_2}{\omega_2} \epsilon(\omega_2) \int dz_2 W[\omega_2(1+z_2), z_2] \\ &\quad \times \frac{2}{\pi} \int dk k^2 P_\delta[k; r(z_1), r(z_2)] j_l[kr(z_1)] j_l[kr(z_2)] \end{aligned}$$

Limber approximation

$$\frac{2}{\pi} \int dk k^2 P_\delta[k; r(z_1), r(z_2)] j_l[kr(z_1)] j_l[kr(z_2)] \simeq \frac{1}{r(z_1)^2} P_\delta\left[k = \frac{l}{r(z_1)}; r(z_1), r(z_2)\right] \delta[r(z_1) - r(z_2)]$$

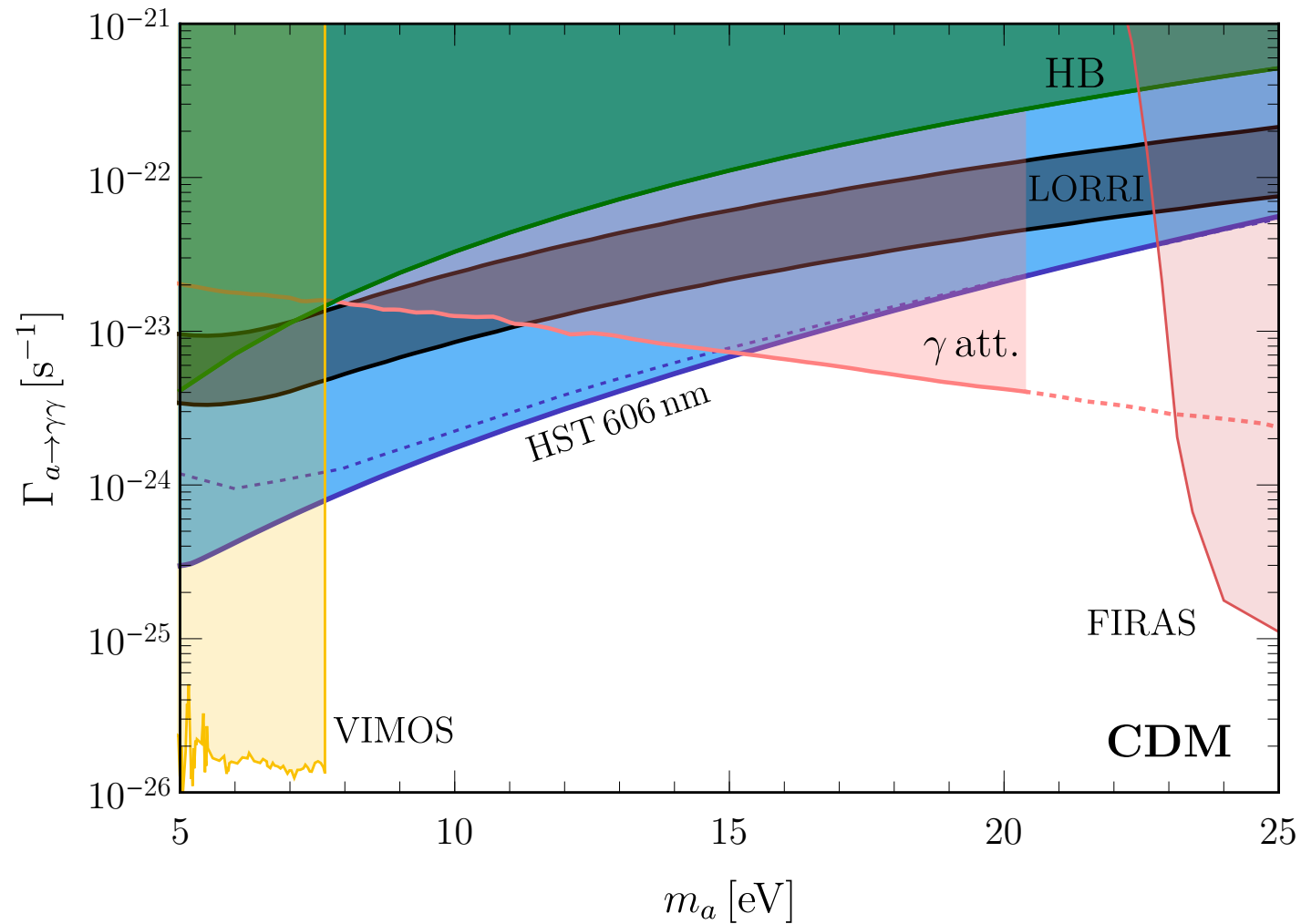
$$C_l(\omega_{\text{piv}}) = \int_0^\infty dz \left[\frac{1}{4\pi} \frac{2 \omega_{\text{piv}}^2 \rho_a}{m_a H(z)} 2 \Gamma_{a \rightarrow \gamma\gamma} \right]^2 \left[\epsilon\left(\frac{m_a}{2(1+z)}\right) \right]^2 \frac{H(z)}{r(z)^2} P_\delta\left[k = \frac{l}{r(z)}, r(z), r(z)\right]$$

BOUND ON CDM



COMPARISON WITH EXISTING BOUND

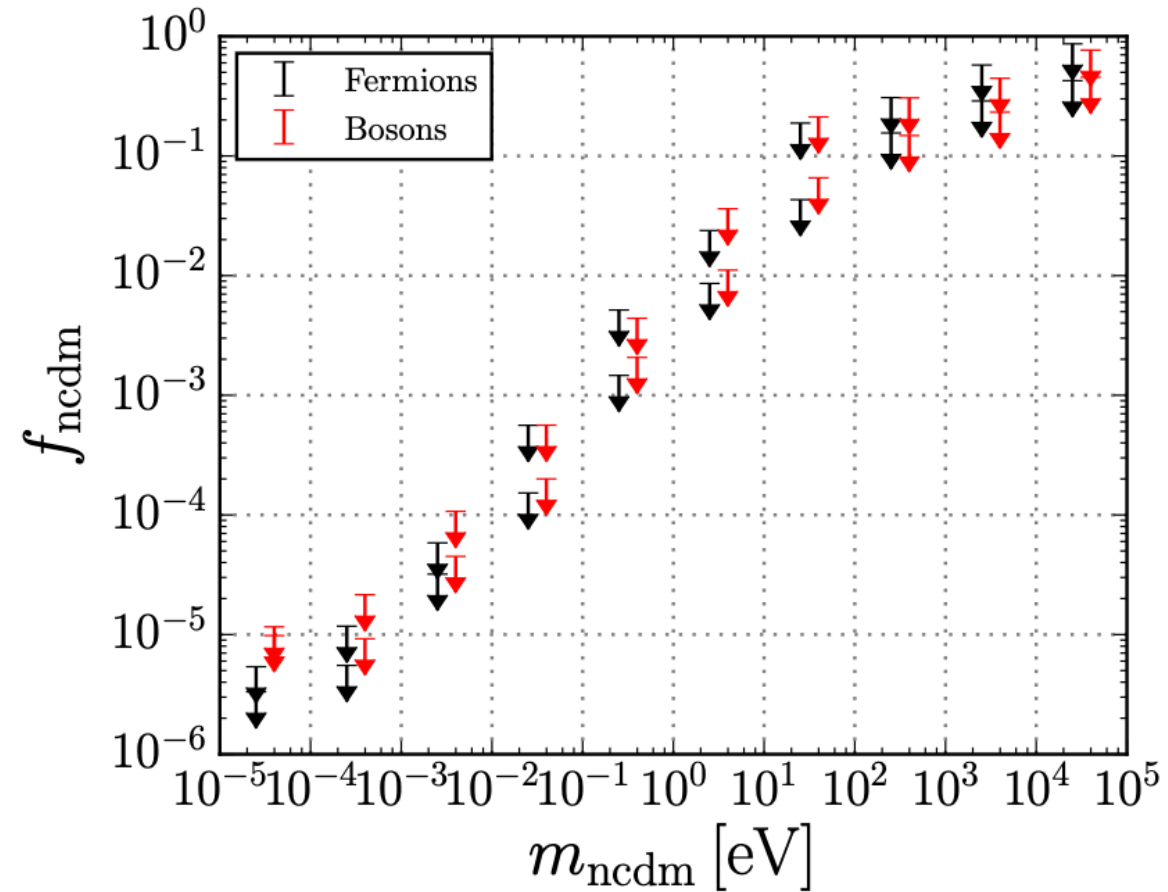
[K. Nakayama & W. Yin, PRD 106 (2022)]



At small masses large discrepancy due to different characterization of the detector.

NCDM FRACTION

[R. Diamanti et al., JCAP 06 (2017) 008]



2σ and 3σ upper limits on the fraction f_{ncdm} of the NCDM component for different ranges of masses. The results are obtained combining CMB + SAT + BAO datasets.

MODIFIED FREEZE-OUT

$$\Omega_a h^2 = \frac{m_a}{13 \text{ eV}} \frac{1}{g_{*,s}(T_F)} \quad \frac{T_a}{T_0} = \left(\frac{g_*(T_0)}{g_{*,s}(T_F)} \right)^{1/3}$$

$$f_{\text{NCDM}} = \frac{\Omega_{\text{NCDM}}}{\Omega_{\text{NCDM}} + \Omega_{\text{CDM}}} \approx \frac{\Omega_{\text{NCDM}}}{\Omega_{\text{CDM}}}$$

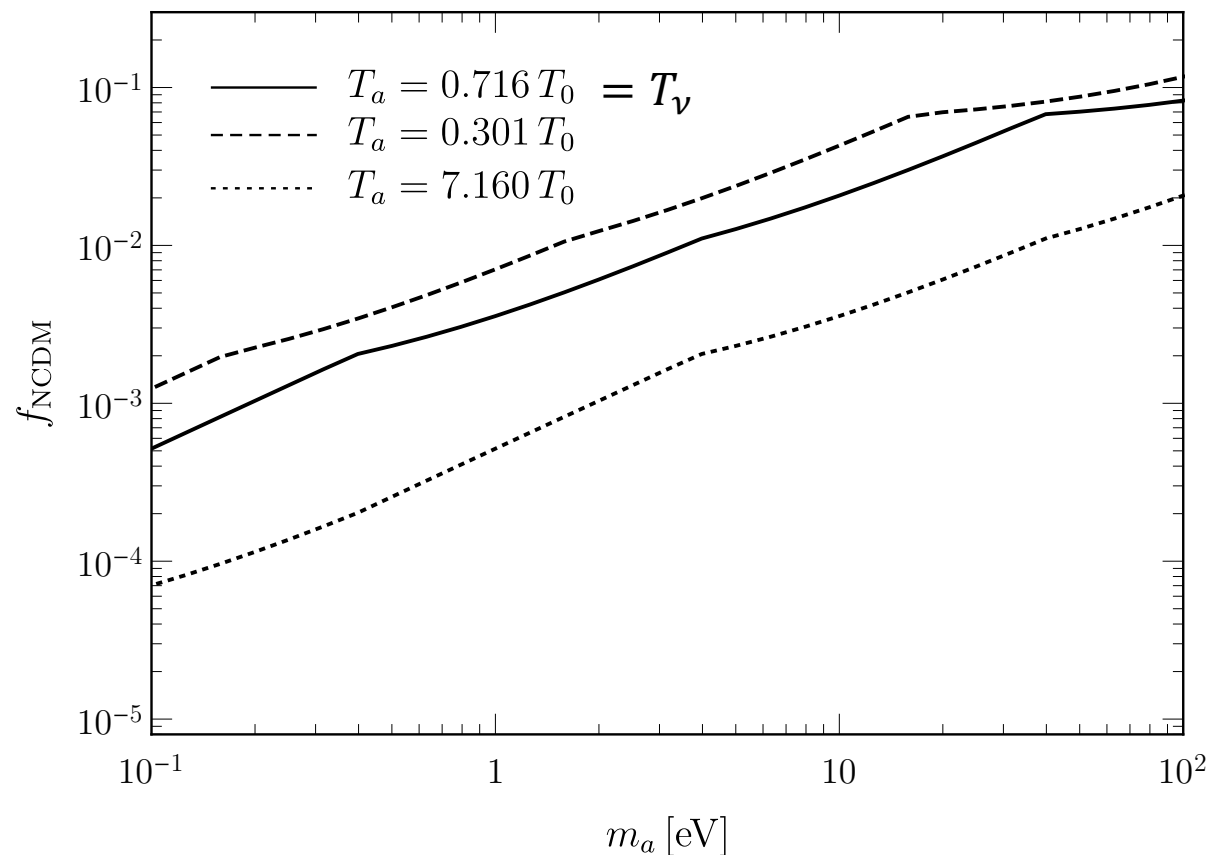
[R. Diamanti et al., JCAP 06 (2017) 008]

Cosmological calculations depend on $\frac{m_a}{T_a}$.

We find the value of $g_{*,s}$ s.t.

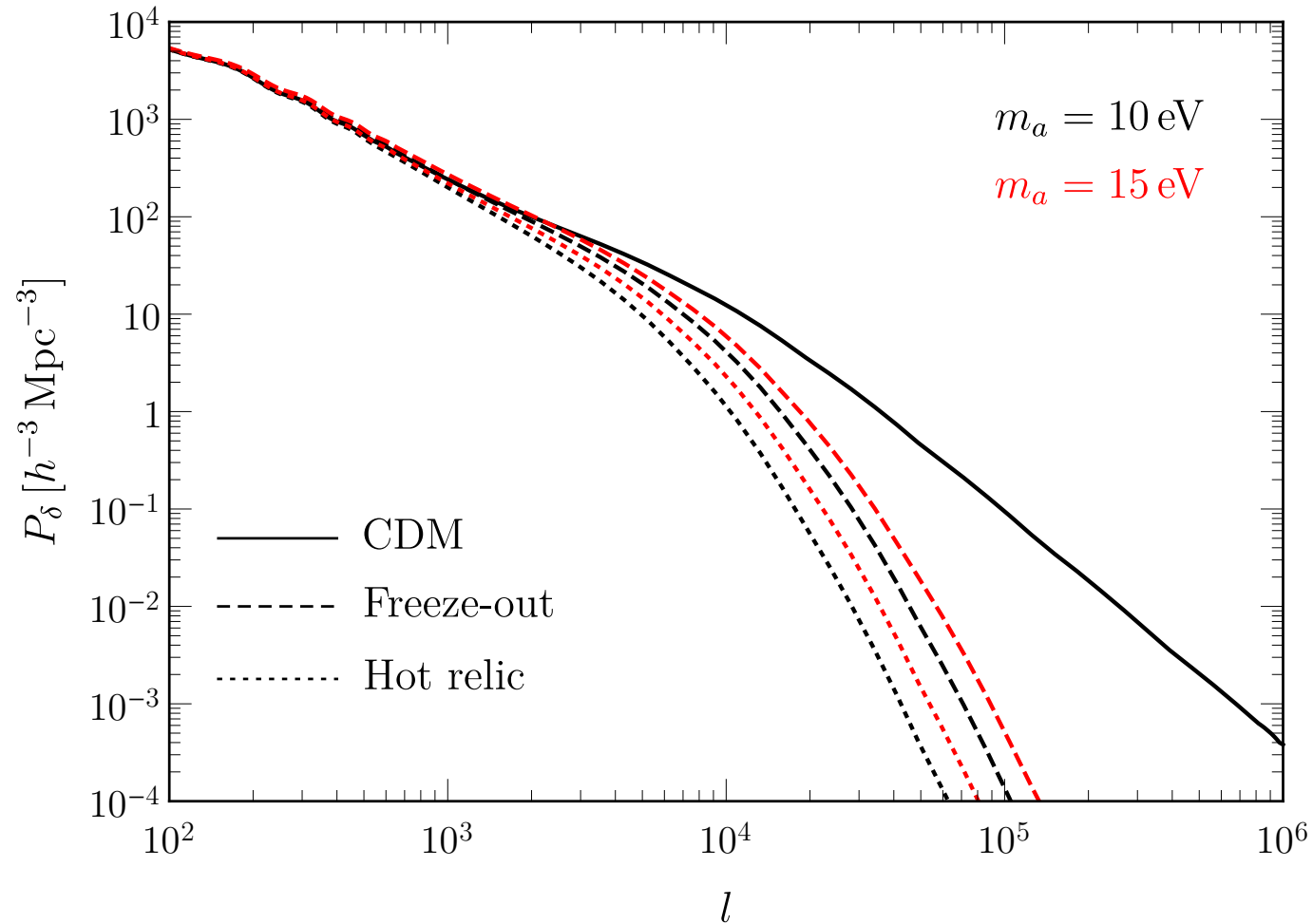
$$\Omega_a h^2 = \Omega_{\text{CDM}} h^2 \frac{f \left[m_{\text{NCDM}} \left(m_a, g_{*,s}(T_F) \right) \right]}{1 - f \left[m_{\text{NCDM}} \left(m_a, g_{*,s}(T_F) \right) \right]}$$

$$m_{\text{NCDM}} \left[m_a, g_{*,s}(T_F) \right] = m_a \frac{T_\nu}{T_0} \left(\frac{g_{*,s}(T_F)}{g_{*,s}(T_0)} \right)^{1/3}$$



THE ROLE OF THE POWER SPECTRUM

$$P_{\delta,\text{NCDM}} = \left(\frac{\mathcal{J}_{\text{NCDM}}}{\mathcal{J}_{\text{CDM}}} \right)^2 P_{\delta,\text{CDM}} \quad [\text{D. Inman \& U.L. Pen, PRD 95 (2017)}]$$



THE DARK PORTAL

[E. Kalashev et al., PRD 99 (2019) 023002]

Let us assume axions can decay through a dark portal featuring a very light dark photon ($m_\chi \ll m_a$)

$$\mathcal{L} \supset \frac{1}{2} g_{a\gamma\chi} a F_{\mu\nu} \widetilde{F}_\chi^{\mu\nu}$$

$$\text{Decay rate: } \Gamma_{a\gamma\chi} = \frac{g_{a\gamma\chi}^2}{32\pi} m_a^3$$

The number of photons produced per unit time is the same for $g_{a\gamma\chi} = g_{a\gamma} = g$.

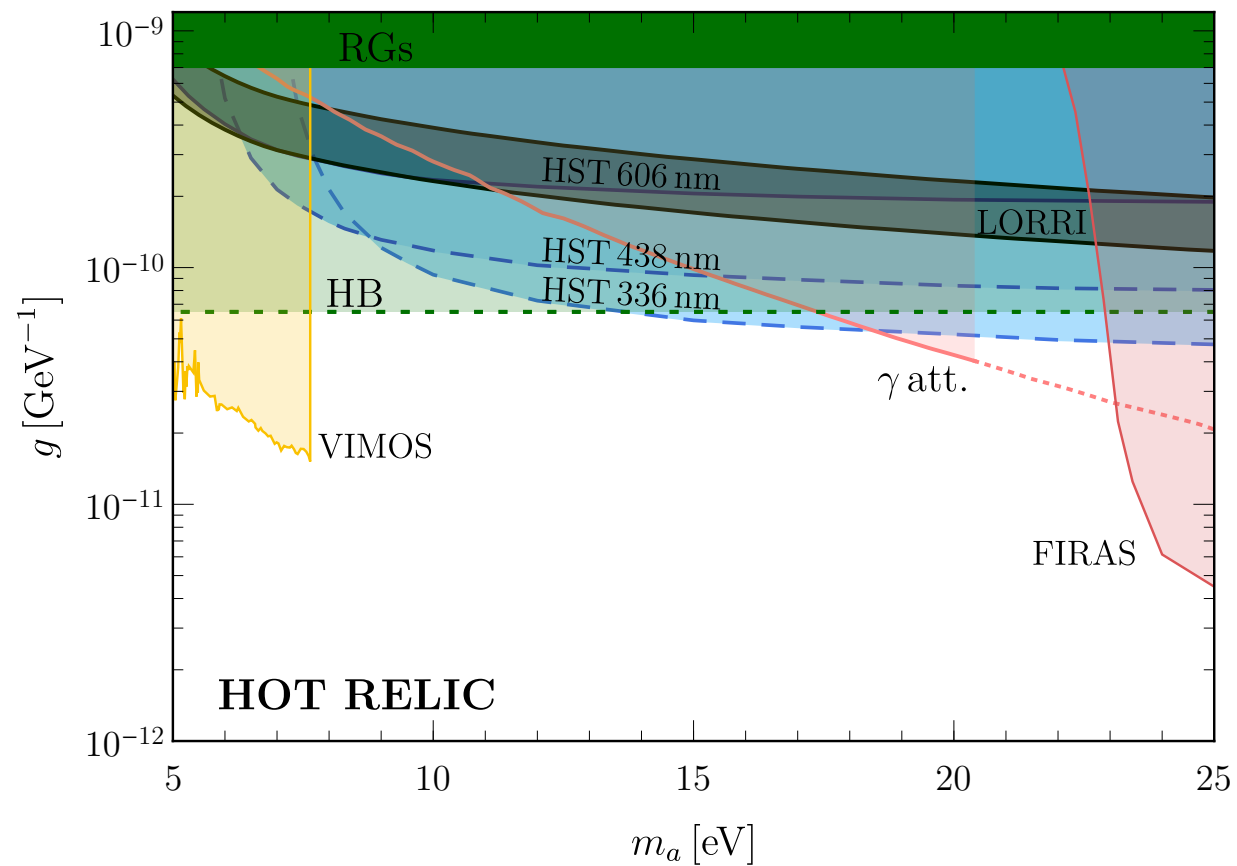
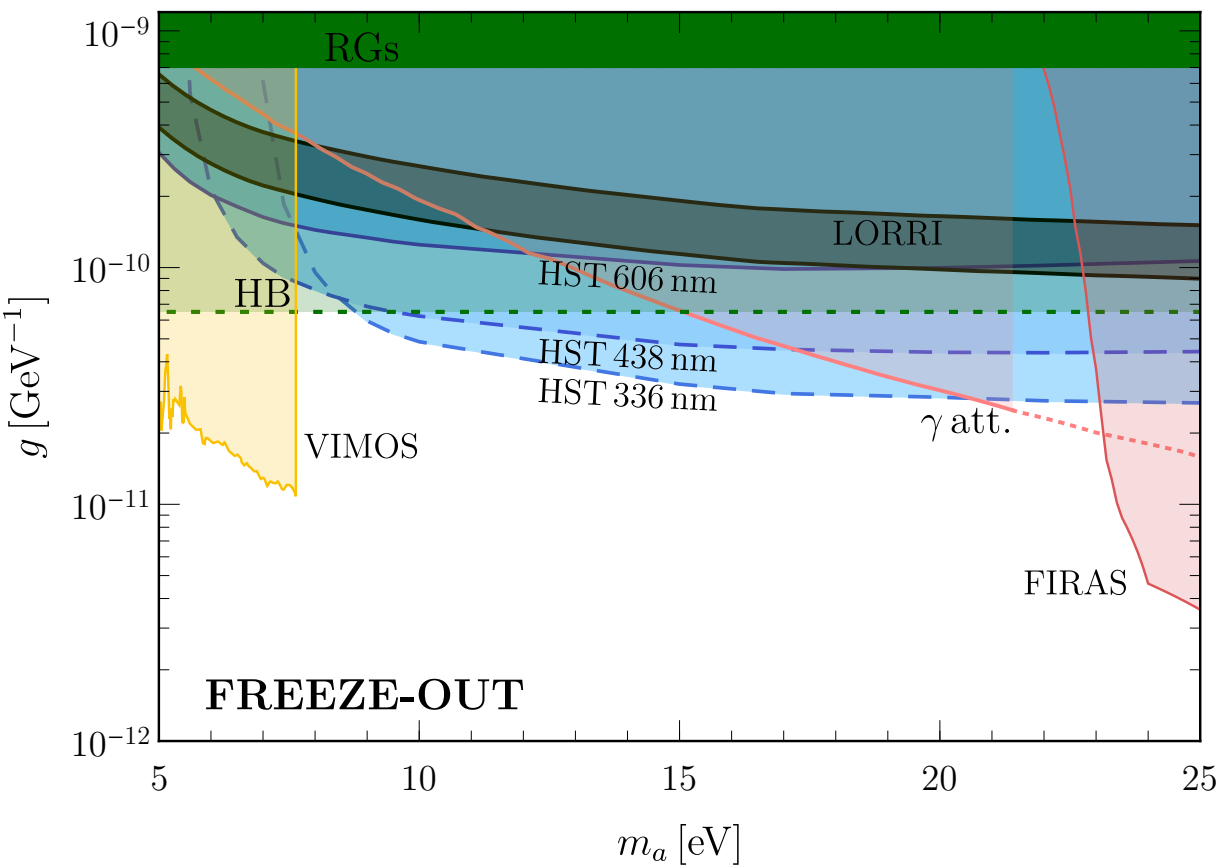
For NCDM, blue axions produced via pair annihilations $e^+ + e^- \rightarrow a + \chi$.

$$T_F \approx 4.8 \times 10^3 \text{ GeV} \left(\frac{g_{a\gamma\chi}}{10^{-9} \text{ GeV}^{-1}} \right)^{-2} \rightarrow T_F > \Lambda_{\text{EW}} \text{ for } g_{a\gamma\chi} \lesssim 10^{-9} \text{ GeV}^{-1}$$

Primakoff emission not possible: no bound from HB stars.

Production via plasmon decay \rightarrow Red Giant bound $g_{a\chi\gamma} < 7.1 \times 10^{-10} \text{ GeV}^{-1}$.

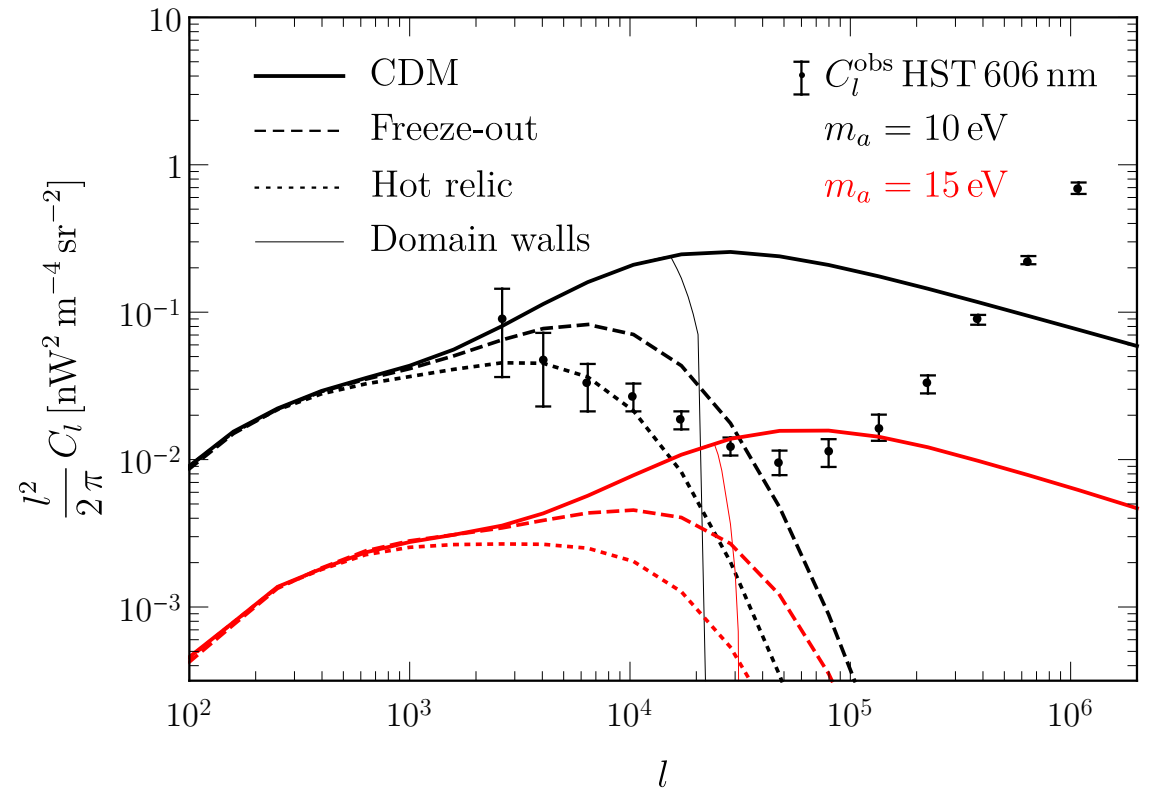
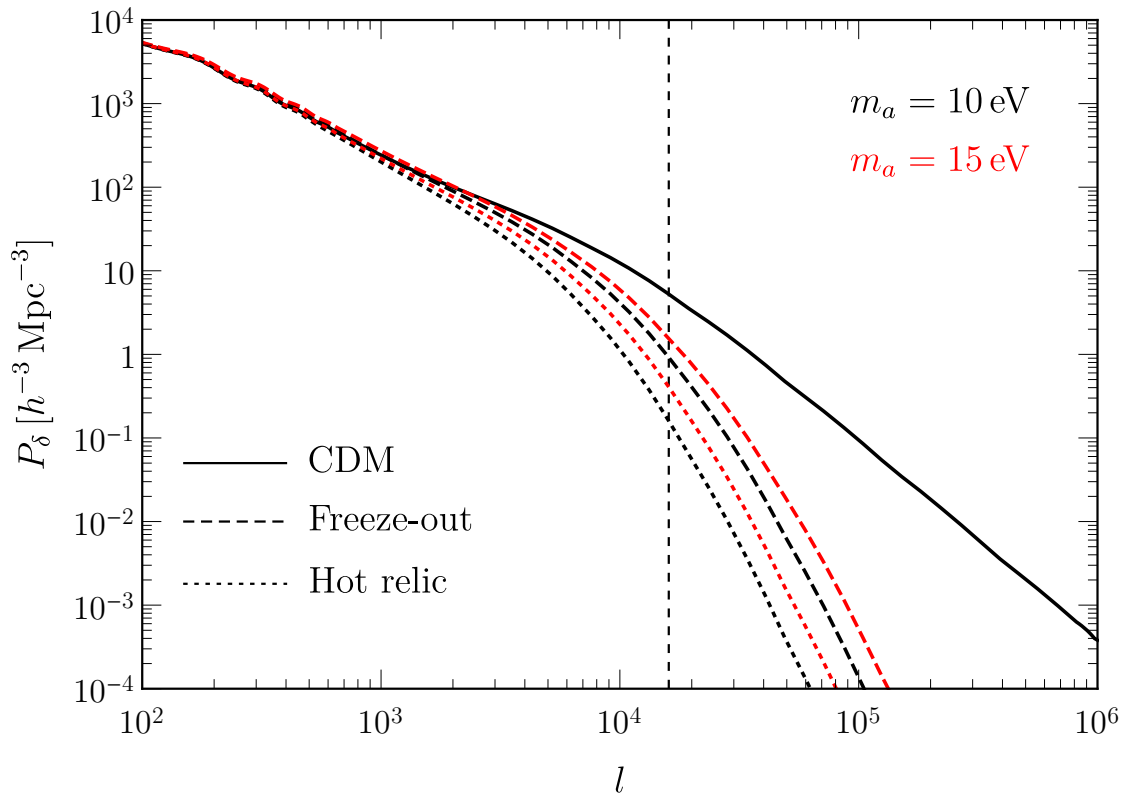
BOUNDS ON NCDM



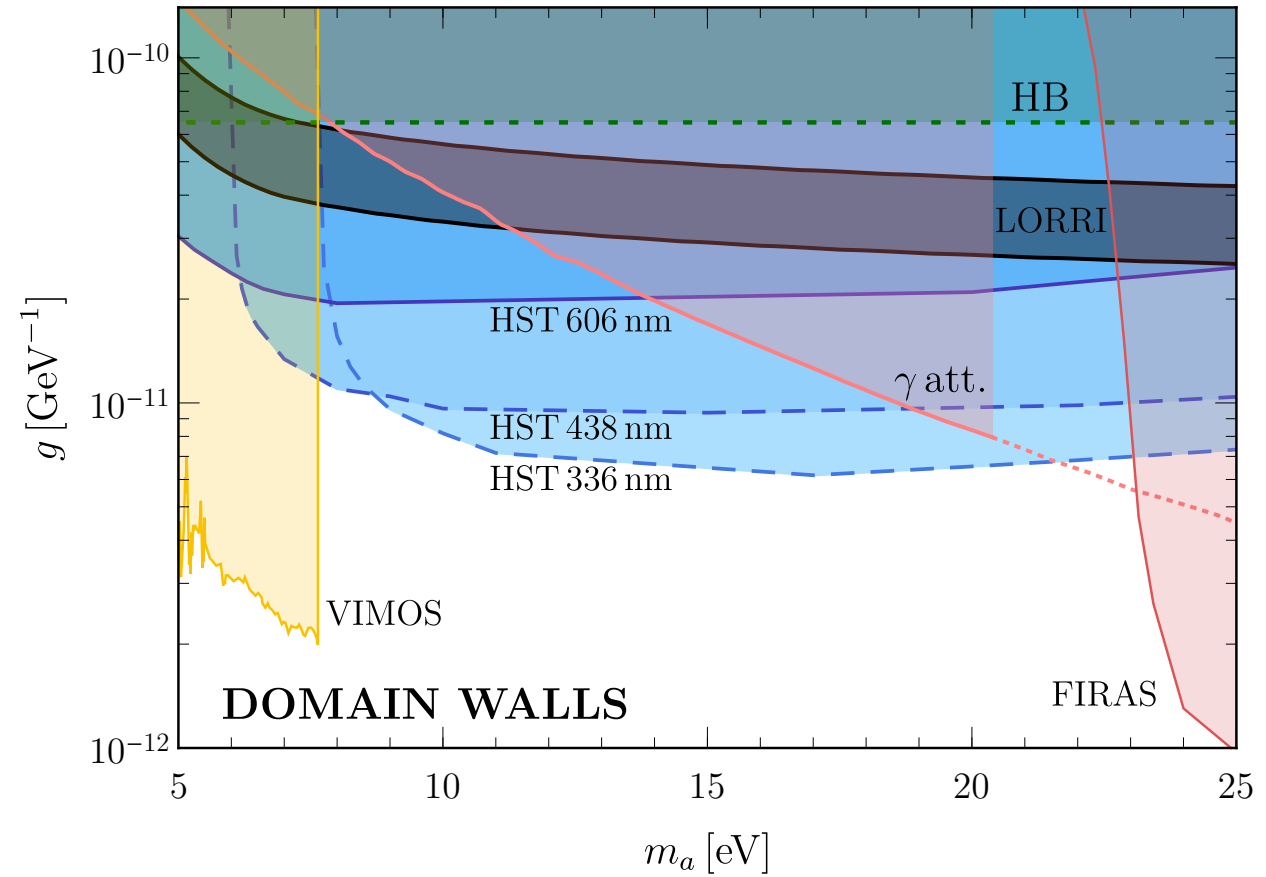
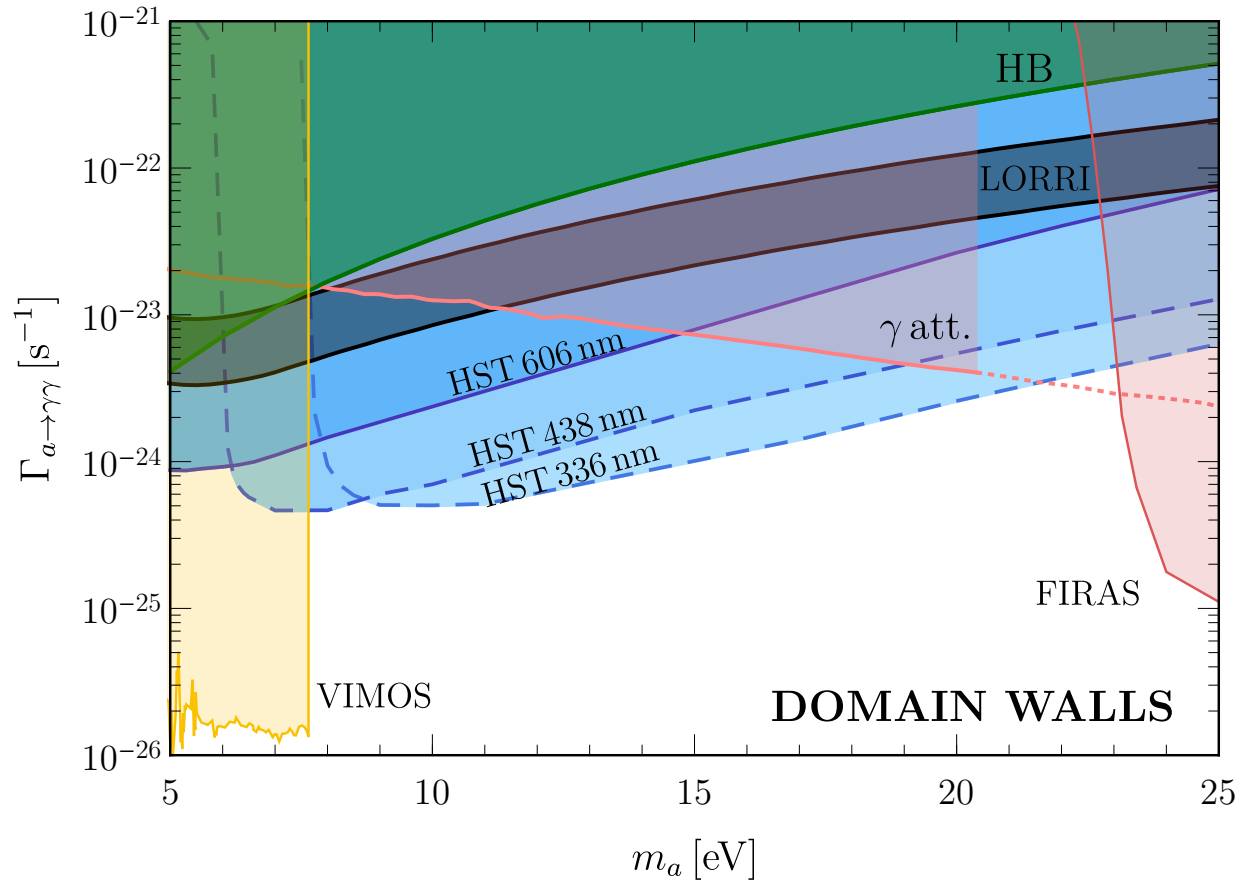
AXIONS FROM DOMAIN WALL DECAY

- $\rho_a = \Omega_{\text{CDM}} \rho_c$, $\Omega_{\text{CDM}} h^2 = 0.12$
- $P_{\delta, \text{CDM}}$ with cutoff at the co-moving wave-number $k_T = 7 h \text{ Mpc}^{-1}$.

[S. Das & E. Nadler, PRD 103 (2021) 043517]



AXIONS FROM DOMAIN WALL DECAY



MODEL CONSTRAINTS

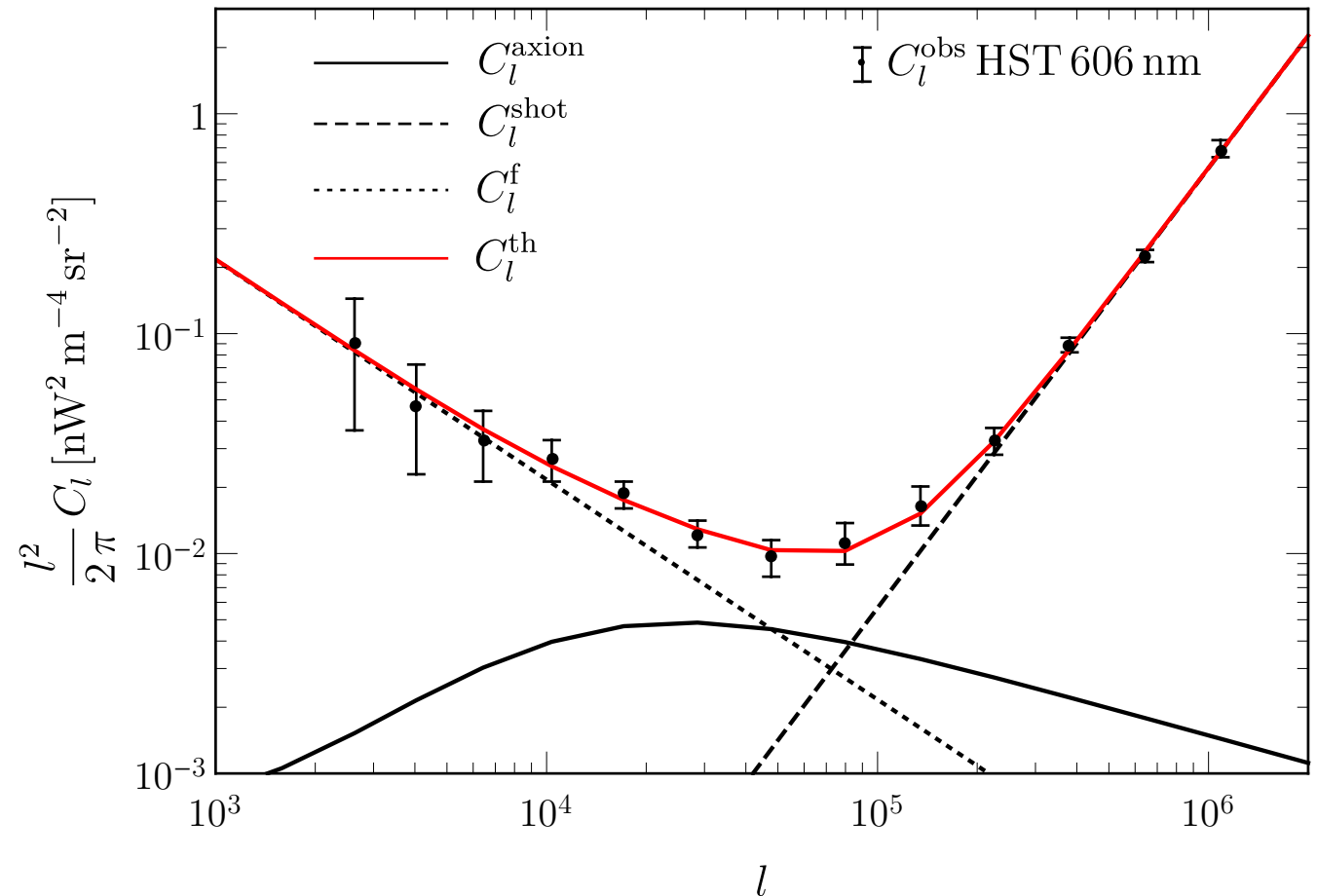
We can model the COB with three main contributions [Y. Gong et al., *Astrophys. J* 825 (2016) 104]

1. Axion-decay contribution C_l^{axion}

2. Shot noise $C_l^{\text{shot}} = A_{\text{shot}}$

3. Galactic foregrounds $C_l^f = A_f l^{-3}$

$$C_l^{\text{th}} = C_l^{\text{axion}} + C_l^{\text{shot}} + C_l^f$$



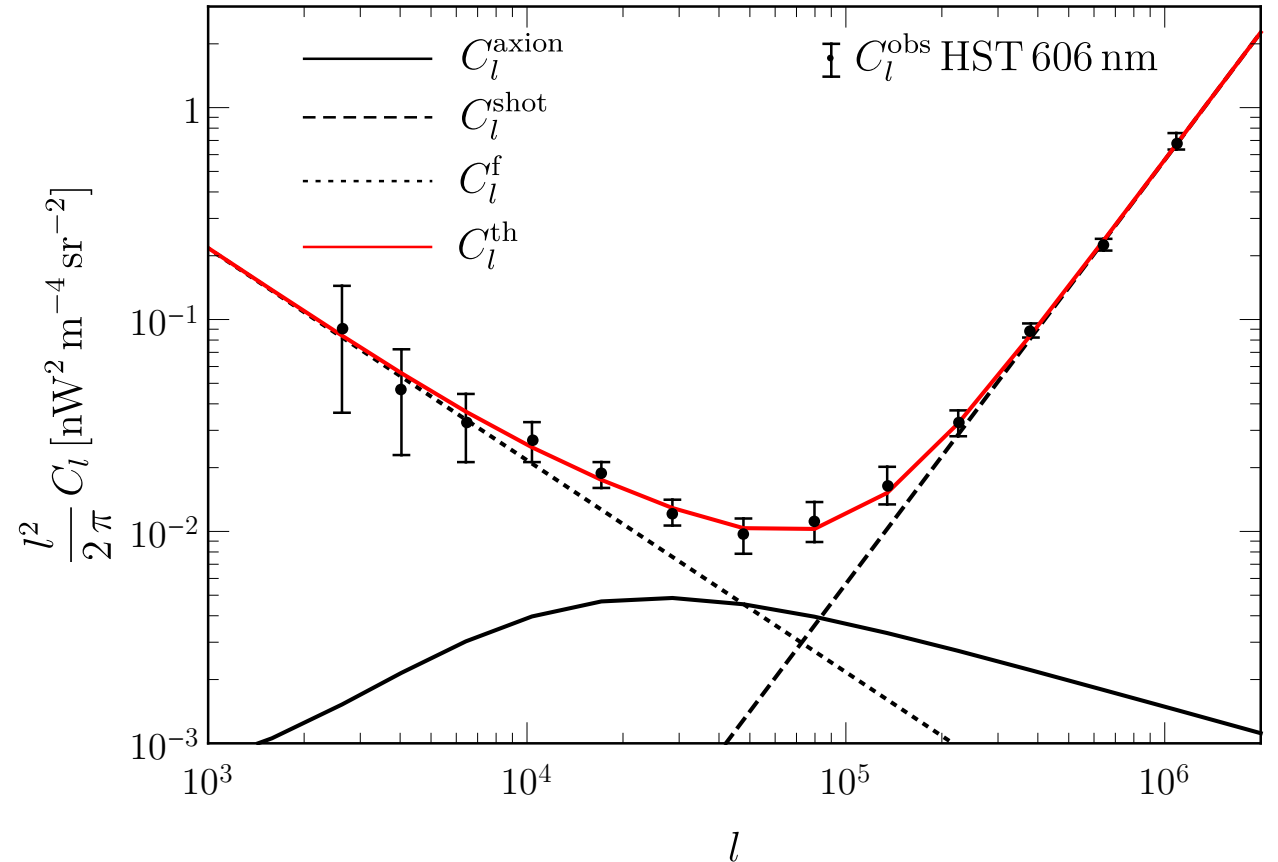
Contribution from high-z faint galaxies negligible. [Y. Gong et al., *Astrophys. J* 825 (2016) 104]

LIKELIHOOD ANALYSIS

$$\chi^2(m_a, g_{a\gamma}, A_{\text{shot}}, A_f) = \sum_{i=1}^{N_d} \frac{(C_{l,i}^{\text{obs}} - C_{l,i}^{\text{th}})^2}{\sigma_i^2}$$

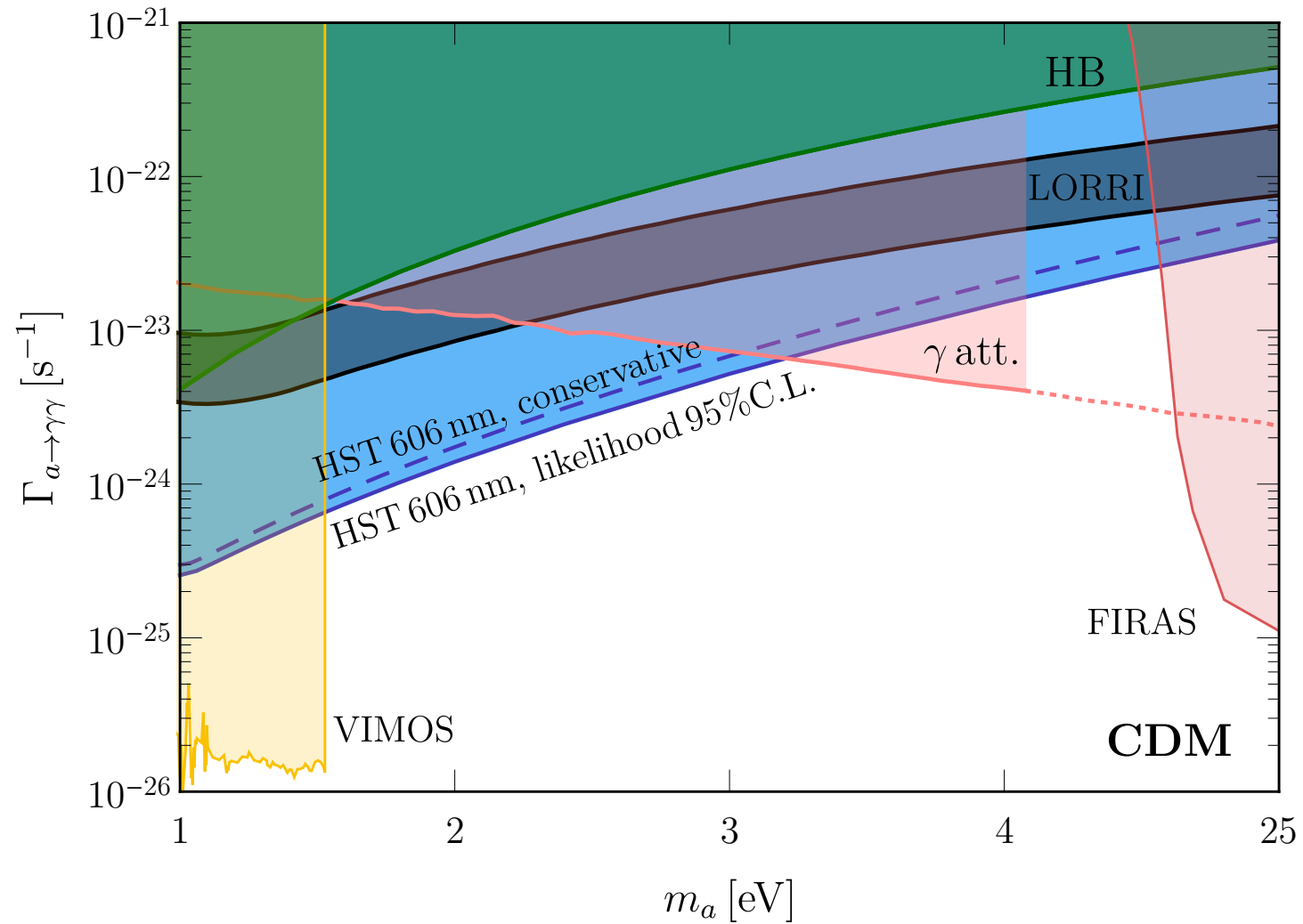
$$\bar{\chi}^2 = \min_{A_{\text{shot}}, A_f} \chi^2(m_a, g_{a\gamma}, A_{\text{shot}}, A_f)$$

$$\chi_*^2 = \begin{cases} \bar{\chi}^2 - \bar{\chi}_{\text{min}}^2 & g_{a\gamma} \geq g_{\text{min}} \\ 0 & g_{a\gamma} < g_{\text{min}} \end{cases}$$

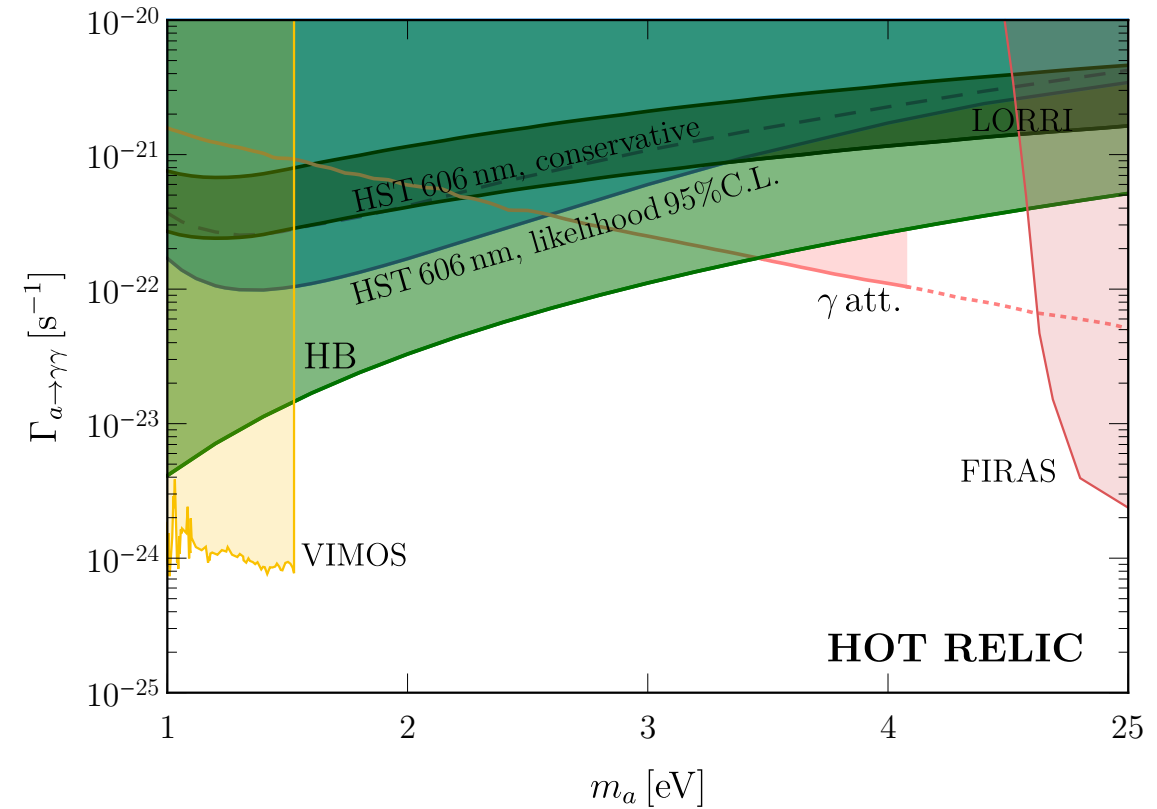
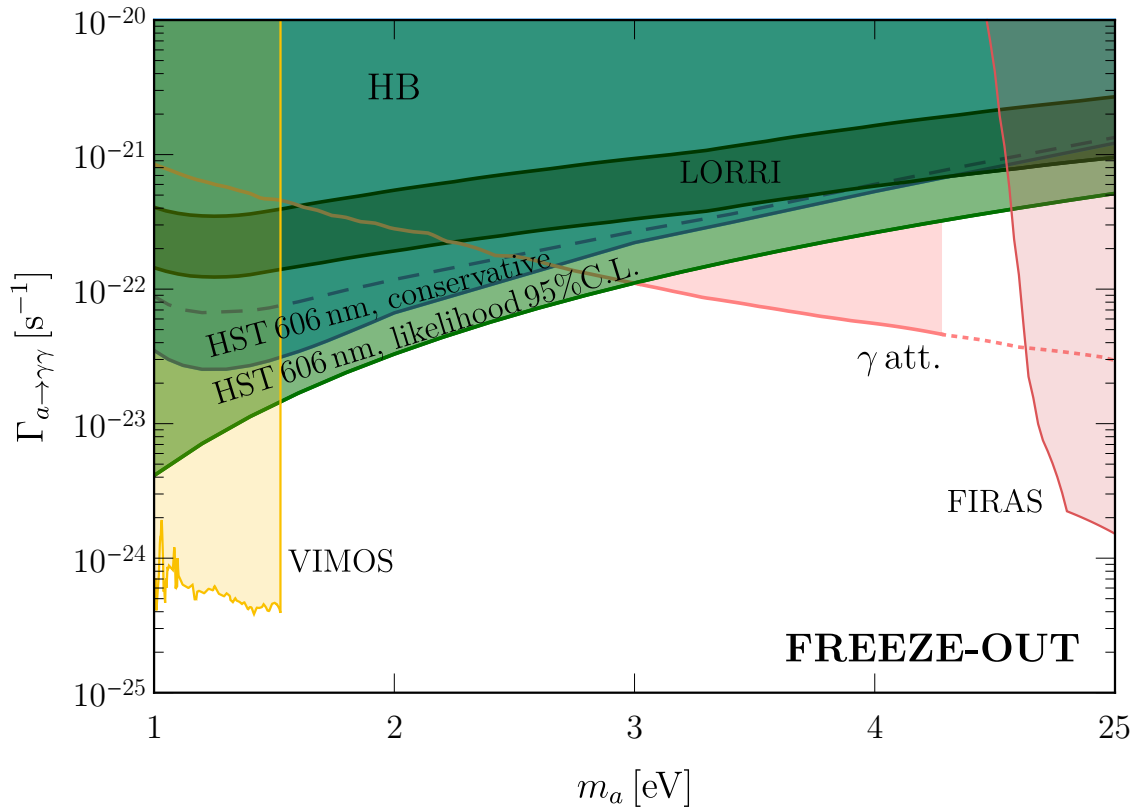


Half-chi square distribution: bound at 95% CL for $\chi_*^2 \leq 2.7$. [G. Cowan et al., Eur. Phys. J C 71 (2011) 1554]

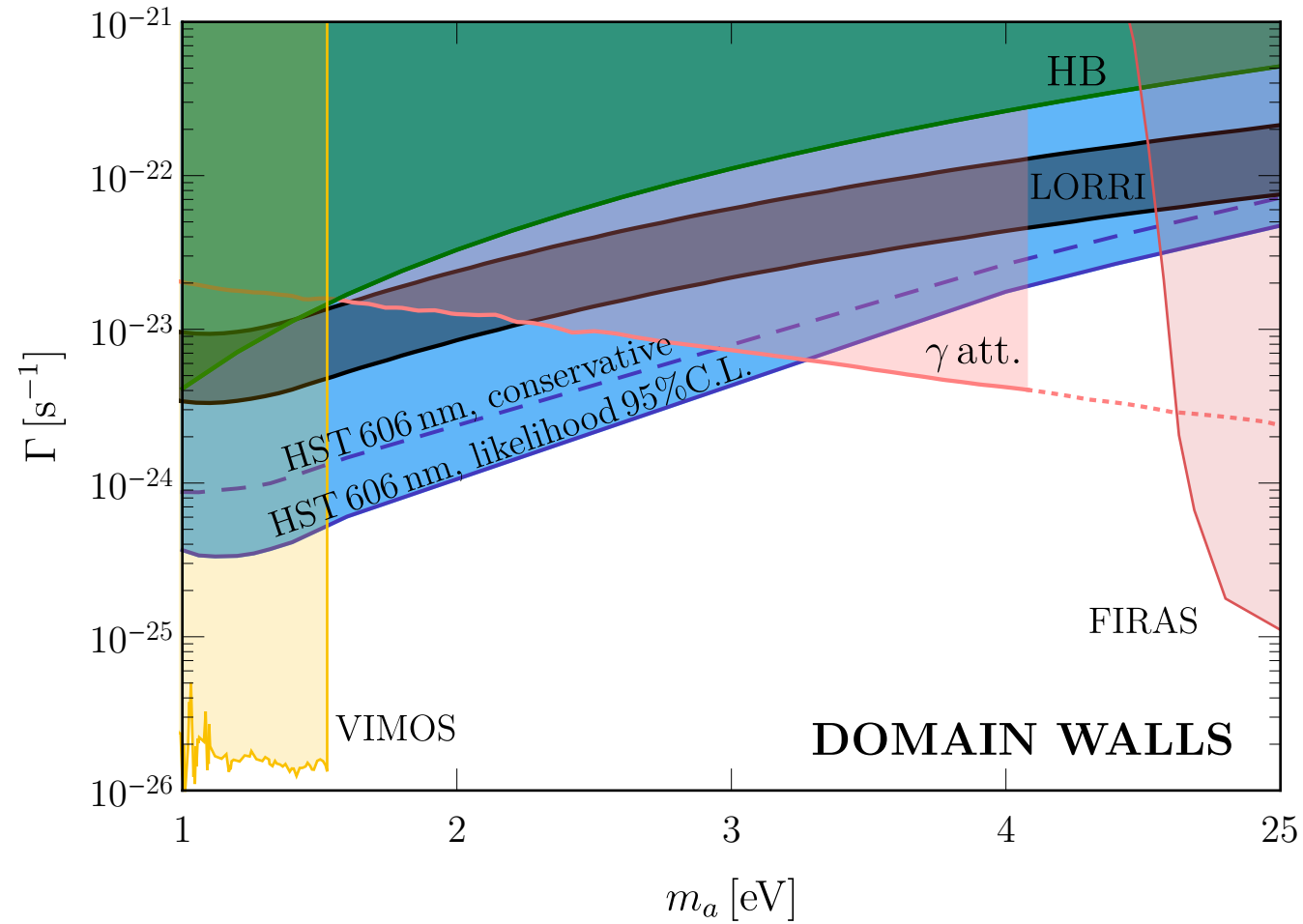
BOUND FROM LIKELIHOOD ANALYSIS



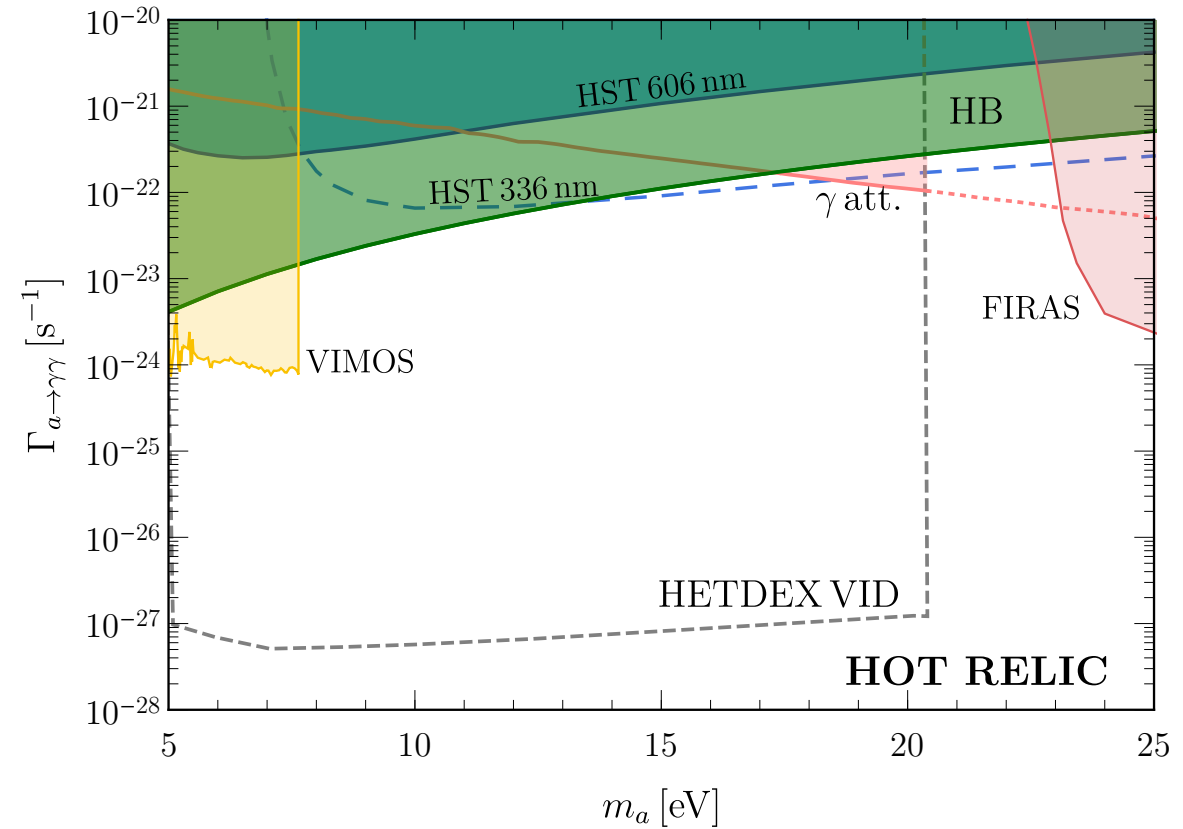
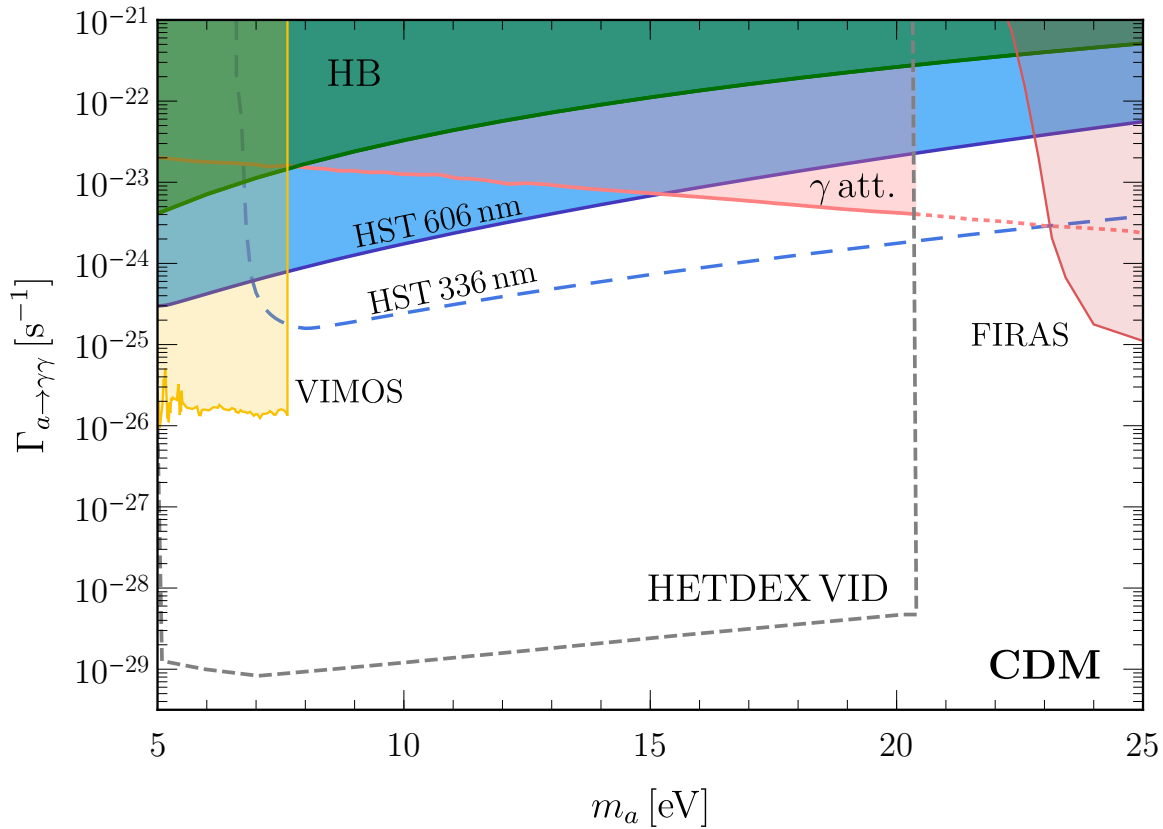
BOUNDS FROM LIKELIHOOD ANALYSIS



BOUNDS FROM LIKELIHOOD ANALYSIS



LINE INTENSITY MAPPING REACHES



Projections from [J.L. Bernal et al., PRD 105 (2022) 089901] rescaled by a factor $\Omega_{\text{CDM}}/\Omega_a$.
LIM experiments can improve current bounds by many orders of magnitude.